Chapter 2

Heterogeneous base catalyst derived from post-harvest *Musa paradisiaca* plant for production of biodiesel

2.1 Introduction

"Banana wastes have wide applications and these have been reported for the production of sugars (Tiwari et al., 2018), biomethane (Wobiwo et al., 2017), biochar (Karim et al., 2017), biogas and bioethanol (Pazmiño-Hernandez et al., 2017). Potassium is one of the major macronutrients which plays a remarkable role in the growth and development of the plant, and it is abundantly found in the post-harvest banana wastes that can be used for K replenishment in the soil (Karim et al., 2017). The water extract of banana ash, being highly alkaline in nature due to the presence of a high percentage of potassium along with other minerals, has been traditionally used as food additives by the people of Assam of North-East India for serving traditional food items (Deka and Talukdar, 2007). *Musa paradisiaca* peel and stalk derived materials have been reported as adsorbents for the removal of fluoride ions (Getachew et al., 2015), malachite green dye (Bello et al., 2012), cadmium (II) and lead (II) ions (Shibi et al., 2006), copper (II) ions (Hasanah et al., 2012), and lead (II) ions (Ogunleye et al., 2014). As per as the literature survey is concerned, only a few reports are available so far on biodiesel synthesis using *Musa paradisiaca* peel catalyst (Betiku and Ajala, 2014; Betiku et al., 2016; Etim et al., 2018). The application of heterogeneous base catalysts derived from *M. paradisiaca* trunk (pseudo-stem) and its rhizome (underground stem) has not yet been reported for the synthesis of biodiesel as well as for any other base-catalyzed reactions. A particular *M. paradisiaca* (Malbhog) plant yields a larger quantity of post-harvest trunk as residues followed by its rhizome compared to the fruit peel. The *M. paradisiaca* trunk and rhizome parts in terms of generated waste have more potential to be studied for various application purposes including the preparation of catalyst for biodiesel production. In this study, comparative catalytic activity studies of the catalysts derived from the *M. paradisiaca* peel, trunk and rhizome for the synthesis of biodiesel from the *Jatropha curcas* oil have been reported for the first time (Basumatary et al., 2021a). The influences of various parameters of the reaction such as catalyst concentration (wt. %), methanol to oil molar ratio (MTOMR), different alcohols, reaction time, activation energy, catalyst reusability, and the properties of biodiesel were investigated and reported.

2.2 Materials and Methods

2.2.1 Materials

M. paradisiaca (Malbhog) peel, trunk and rhizome were obtained for catalyst preparation from the Dotma (Simlaguri) of Kokrajhar, Bodoland Territorial Region, India in June 2019. *J. curcas* oil for transesterification was purchased from Sinhal Herbs (LIFERR^{TM} Naturally Elite), Madhya Pradesh, India. Acetone (99 %) and petroleum ether (40–60 ^{o}C) were obtained from Rankem, Maharashtra, India. Ethyl acetate (≥ 99.5 %), methanol (≥ 99.0 %), ethanol, 1-propanol, *n*-hexane, anhydrous Na_2SO_4 (≥ 99.0 %), bromothymol blue, aniline, phenolphthalein and silica gel G for thin layer chromatography were purchased from Merck, Mumbai, India. Distilled water was prepared in the laboratory. Benzoic acid was obtained from Avantor Performance Materials India Limited, nile blue from Sisco Research Laboratories, Mumbai, India and 4-nitroaniline from Loba Chemie, Mumbai, India.

2.2.2 Methods

2.2.2.1 Catalyst preparation

After harvesting, *M. paradisiaca* (ripened) peel, trunk, and rhizome were sectioned and separately cut into small pieces, and then allowed to dry under the sunlight for about ten days (**Fig. 2.1**). The dried materials were then ignited separately and burnt to ash materials completely in the open air and it is named ‘burnt material’. The materials obtained were further heated in the furnace for 2 h at 550 ^{o}C, stored in the desiccator, and then milled to fine powders. The powdered materials obtained were stored in an air-tight container, characterized, and applied as the catalyst in the reaction of biodiesel synthesis.

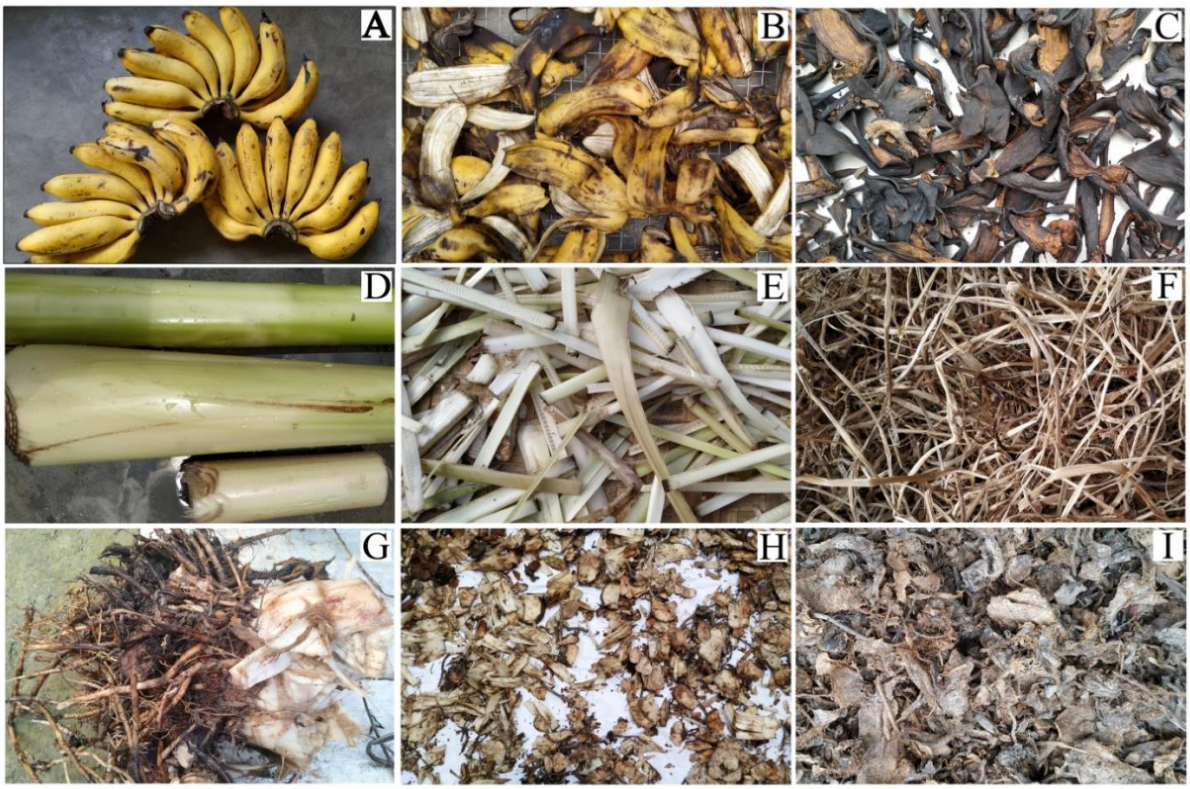

Fig. 2.1. *M. paradisiaca* peel (A–C), trunk (D–F) and rhizome (G–I) used in the preparation of catalyst.

2.2.2.2 Characterization of catalysts

M. paradisiaca catalysts were characterized to investigate the qualitative chemical compositions using powder XRD (Rigaku Ultima-IV) in the Department of Chemistry, Gauhati University, India. The presence of various functional components in the catalyst was characterized by FT-IR spectrometer (Bruker, Alpha II, 410025, Germany) using KBr pellets in the region of 4000–400 cm^{-1} in the Department of Chemistry, NEHU, Shillong, India. BET results were obtained using Quantachrome ASiQwin^{TM} version 3.0 under N_2 atmosphere from Material Analysis and Research Center, Bangalore, India. To study the surface morphology and elemental compositions of the catalysts, FESEM images, and EDX spectra were recorded in Carl Zeiss: ΣIGMA instrument (SIGMA HV, 05–07, UK) at CSIR-NEIST, Jorhat, India. XPS spectra were recorded on the ESCALAB Xi^+ XPS instrument (Thermo Fischer Scientific, USA) to study the surface composition of the catalyst at CSIR-NEIST, Jorhat, India. The structural information of the *M. paradisiaca* catalyst was investigated from the HRTEM images and selected area electron diffraction (SAED) patterns obtained from the HRTEM instrument (JEOL, JEM2100 plus) at CSIR-NEIST, Jorhat, India.

To determine the pH value of *M. paradisiaca* catalyst (calcined at 550 ^{o}C), it was dissolved with water (distilled) in the ratios of 1:5, 1:10, 1:15, 1:20, 1:30, 1:40 (w/v), and pH value was tested using Auto deluxe digital pH meter (LT10).

The elemental analysis of the liquid samples of *M. paradisiaca* catalysts at 1:5 w/v was carried out. The analysis of Na and K was done by Flame Photometer (Systronics-128), Ca, Mn and Fe by AAS (Shimadzu-AA-6300), P by double beam UV-Visible spectrophotometer (Systronics-2203) and Cl by titration method.

Soluble alkalinity values of the calcined *M. paradisiaca* catalysts (peel, trunk and rhizome) were determined following the procedure reported by Mendonça et al. (2019a) with slight modification. The weighed catalyst (0.5 g) was dispersed in 50 mL of distilled water taken into a conical flask. The solution was allowed to stir for 48 h over a magnetic stirrer at room temperature. Thereafter, the solution was filtered through Whatman grade no.1 filter paper. The filtrate was titrated against the 0.1 M solution of HCl using a digital pH meter. The records of the initial pH of each filtrate were taken and then neutralized to pH 7 observing the burette reading. The soluble alkalinity was calculated based on the number of mmol HCl required in neutralizing 1 g of the leached *M. paradisiaca* catalyst in the solution.

The basicity of the *M. paradisiaca* catalyst was estimated following the benzoic acid titration method using the Hammett indicator (Roy et al., 2020b). Methanolic solutions (0.02 mol/L) of aniline (H_ = 27.0), 4-nitroaniline (H_ = 18.4), nile blue (H_ = 10.1), phenolphthalein (H_ = 9.3) and bromothymol blue (H_ = 7.2) were used as indicators. In a conical flash of 50 mL, 100 mg of *M. paradisiaca* catalyst was thoroughly mixed with 15 mL methanol and the solution was stirred with the magnetic stirrer for 2-3 min. The indicator (2-3 drops) was added to the solution, stirred for 30 min, and thereafter it was kept for about 15 min to reach the equilibrium. The change in color of the solution was recorded. The solution was then titrated against 0.01 molar solution of the benzoic acid prepared in methanol. The titre value recorded in titration indicated the requirement of benzoic acid in millimole (mmol) to neutralize 100 mg of the catalyst used in the experiment, and the basicity of the catalyst was determined in mmol g^{-1}.

2.2.2.3 Transesterification and characterization of biodiesel

The transesterification of *J. curcas* oil (2 g) was performed in a two-neck round-bottom flask (100 mL) connected to a reflux condenser and fitted with a hot-plate magnetic stirrer using a speed of 650-680 rpm to produce biodiesel with methanol using the three different catalysts (*M. paradisiaca* peel, trunk and rhizome) at different reaction temperatures (32, 45,

55, 65 and 75 ^{o}C). The optimum conditions of the reaction were examined by varying the concentration of catalyst (3, 5, 7 and 9 wt. % of oil) and using different MTOMR (3:1, 6:1, 9:1, 12:1, 15:1 and 18:1). The reaction was also investigated using different alcohols such as ethanol and 1-propanol. Thin layer chromatography (solvent system, 1:20 v/v of ethyl acetate and petroleum ether) was used to monitor the complete transformation of oil to biodiesel. After completion of the reaction, the catalyst was filtered through Whatman no. 42 using a suction pump. Petroleum ether (40–60 ^{o}C) was used to extract the produced biodiesel. In a separating funnel containing the product mixtures, petroleum ether (6 mL) was added followed by the addition of 10 % NaCl solution (3 mL) with constant shaking. The solution was kept till the appearance of two distinct layers. The upper layer containing the biodiesel was collected, and the extraction is repeated four to five times. The extracted biodiesel was dried over Na_2SO_4 (anhydrous) and the solvent was completely removed using a rotary evaporator (QuickVap, Almicro) at 50 ^{o}C. The yield of biodiesel was calculated by applying equation (**2.1**).

$$\text{Yield of biodiesel (\%)} = \frac{\text{Weight of biodiesel}}{\text{Weight of oil taken for reaction}} \times 100 \qquad (\mathbf{2.1})$$

To study the changes of absorption bands in transesterification of *J. curcas* oil to biodiesel, the samples were analyzed using FT-IR spectrometer (Shimadzu, MIRacle 10, 00644). The *J. curcas* oil and synthesized biodiesel were characterized by the ^{1}H and ^{13}C NMR spectra recorded with FT-NMR spectrometer in 400 MHz and 100 MHz (Bruker Avance II) at NEHU, Shillong, India using $CDCl_3$ as the solvent. The biodiesel obtained was investigated to know the methyl esters of different fatty acids using Perkin Elmer GC-MS (Clarus 600, Elite 5 MS, 123.5 m × 678 µm, split ratio = 20:1, mass scan = 20 to 500 Da) in the Department of Chemistry, Gauhati University, Assam, India. The initial temperature was maintained at 90 ^{o}C for 3 min during analysis. The temperature is ramped at 10 ^{o}C/min to 130 ^{o}C, held for 3 min, ramped at 10 ^{o}C/min to 210 ^{o}C, it was held for 5 min, and again ramped at 15 ^{o}C/min to 280 ^{o}C. Helium was the carrier gas, source temperature was 150 °C and transfer temperature was 180 °C. Properties of jatropha biodiesel such as cetane number, cold filter plugging point, pour point, kinematic viscosity, and density were tested at Indian Oil Corporation Limited, Bongaigaon, India. Other biodiesel properties such as saponification number (SN) and iodine value (IV) were measured by the empirical equation (Barua et al., 2014; Basumatary et al., 2014) mentioned below.

$SN = \Sigma (560 \times A_i)/MW_i$ and $IV = \Sigma (254 \times D \times Ai)/MW_i$

Where, A_i = percentage composition of individual component, MW_i = the molecular mass of individual component and D = the number of double bonds in an individual component.

In addition, higher heating value (HHV), American petroleum index (API), cetane index (CI), aniline point and diesel index (DI) were calculated using standard equations recognized by American Society of Testing and Materials (ASTM) D2015 (Adepoju et al., 2018).

$HHV = 49.43 - [0.041(SN) + 0.015(IV)]$

$API = (141.5/\text{Specific gravity at } 15\ ^oC) - 131.5$

$CI = 46.3 + (5458/SN) - 0.225IV$

$AP = (DI \times 100)/API$

$DI = (CI - 10)/0.72$

2.2.2.4 Activation energy determination

The transformation of oil (triglyceride) to its biodiesel via transesterification with the excess amount of methanol was reported to follow the kinetics of pseudo-first-order reaction (Kaur et al., 2018). In this study, *M. paradisiaca* peel, trunk, and rhizome catalyzed transesterification reactions of *J. curcas* oil were investigated at various reaction temperatures (32, 45, 55, 65 and 75 ^oC), the values of rate constants were determined by following the equation mentioned below.

$-\ln (1-X_{FAME}) = k.t$

where, X_{FAME} is the yield of produced biodiesel at time 't'.

The activation energies were calculated using the Arrhenius equation (Nath et al., 2019) mentioned below.

$\ln k = - Ea/RT + \ln A$

where, 'R' is the universal gas constant (8.314 J K^{-1} mol^{-1}), 'T' is the reaction temperature in Kelvin and 'A' is the pre-exponential factor.

2.3 Results and Discussion

2.3.1 Catalyst characterization

2.3.1.1 Powder XRD analysis

The qualitative crystalline chemical components of the calcined *M. paradisiaca* peel, trunk, rhizome, and 3rd recycled trunk catalysts are probed from the XRD patterns (**Fig. 2.2**) by comparing the 2θ values with JCPDS (Joint Committee on Powder Diffraction Standard, ICDD 2003) data and reported literature. The investigation reveals the presence of mixed metal oxides and carbonates along with potassium chloride and calcium hydroxide in the catalysts. The components of potassium were found to be abundant in all three catalysts. The 2θ values at 29.68, 32.19, 32.69, and 41.50 in the peel catalyst, 26.63, 29.66, 30.94, 31.90, 33.79, 41.27, and 41.60 in trunk catalyst, and 26.65, 29.65, 31.59, 33.86, 41.35, and 41.63 in the rhizome catalyst showed the abundance of K_2CO_3. Comparable 2θ values of K_2CO_3 were reported by Nath et al. (2019; 2020) in *Brassica nigra* and *Sesamum indicum* catalysts which are supporting the results of this study. Gohain et al. (2017) reported identical 2θ values of K_2CO_3 in *M. balbisiana* peel catalyst that was studied in transesterification. The presence of KCl in the *M. paradisiaca* catalysts is represented by the 2θ values at 28.41, 40.53, 50.22, 58.64, 73.67 in peel catalyst, 28.34, 40.49, 49.29, 50.15, 58.61, 73.67 in trunk catalyst, and 28.36, 40.53, 50.13, 73.80 in rhizome catalyst. These values are well comparable with the reported 2θ values in the works of Nath et al. (2019; 2020). Comparable peaks for KCl were also observed in the waste banana peel catalyst reported by Fan et al. (2019). The peaks at 2θ values of 27.93, 39.73, and 48.16 in trunk catalyst and 27.96 in rhizome catalyst are due to K_2O present in the catalysts (Nath et al., 2019). Various components of Ca like CaO, $CaCO_3$ and $Ca(OH)_2$ were characterized by XRD (**Fig. 2.2**). These are supported by the results reported in the works of Nath et al. (2019) and Jin et al. (2017). The existence of SiO_2 in the catalysts is identified by the peaks at 2θ value of 25.88 (peel), 25.71 (trunk) and 25.45 (rhizome). SrO present in the catalysts is shown by the peaks at 2θ value of 62.29 (peel), 30.70, 62.80 (trunk), and 29.74, 65.64 (rhizome). Na in the form of Na_2O showed XRD peak at 2θ value of 32.08 in the trunk catalyst and 32.14 in the rhizome catalyst. This is in accordance with the value reported by Nath et al. (2020). The presence of Fe_2O_3 in trunk and rhizome catalysts is represented by the peaks at 23.74 and 32.63 in the trunk, and 32.92 in the rhizome catalyst. The XRD pattern (**Fig. 2.2**, red line) of the 3rd recycled trunk catalyst also indicated the presence of K_2CO_3, K_2O, KCl, MgO, $CaCO_3$ and CaO in the recycled material. Conclusively the powder XRD study revealed the presence of carbonates and oxides of various metals. The potassium (K) being the abundant

component in the form of its carbonate, oxide and chloride in the present catalyst played a significant role in the transformation of *J. curcas* oil.

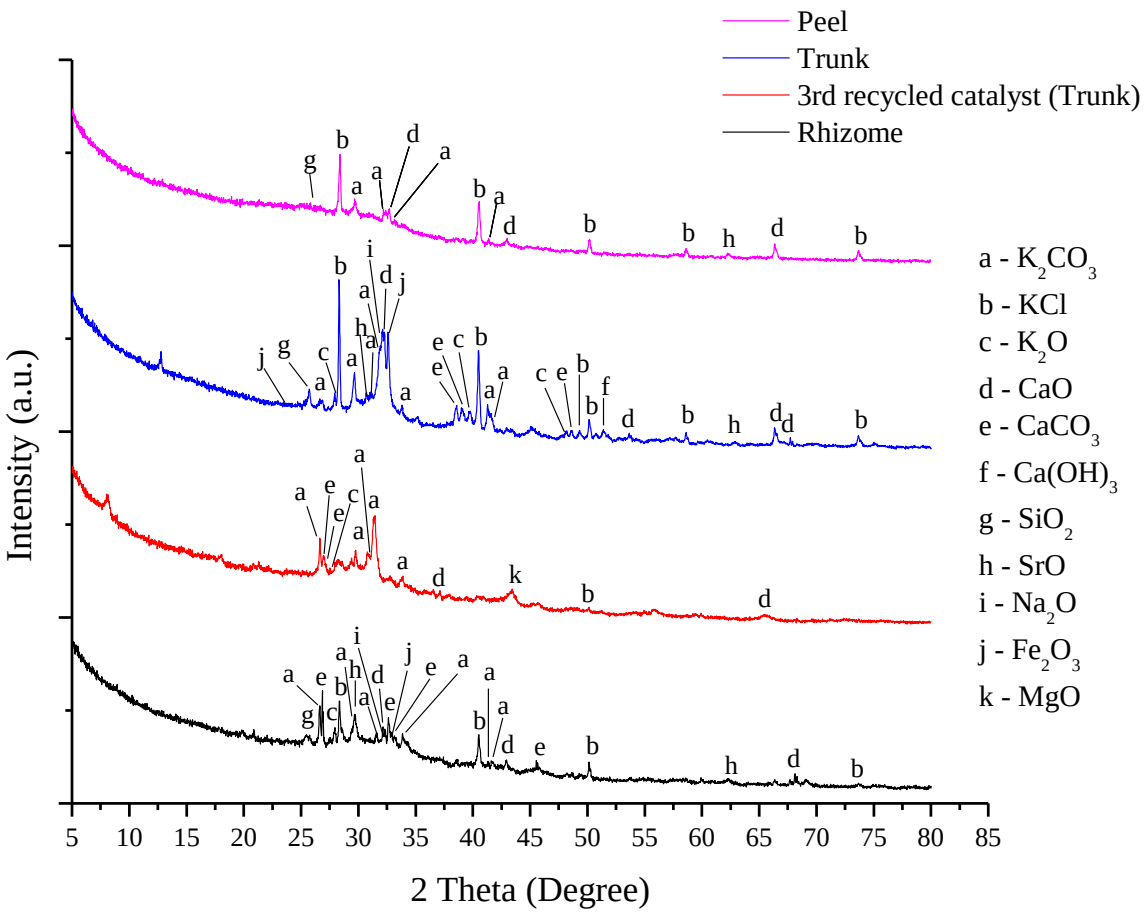

Fig. 2.2. XRD patterns of calcined *M. paradisiaca* catalysts.

2.3.1.2 FT-IR analysis

The FT-IR spectra (**Fig. 2.3**) of calcined *M. paradisiaca* catalysts were recorded to study the vibrational frequencies of various functional components. The surface of the catalyst adsorbed by the H_2O molecules is represented by the broad IR peak at 3441 cm^{-1} (peel), 3456 cm^{-1} (trunk), 3447 cm^{-1} (3^{rd} recycled trunk catalyst) and 3448 cm^{-1} (rhizome). The peaks observed at 1643, 1466 and 1402 cm^{-1} in the spectra of the three catalysts, and the peaks at 1639, 1491 and 1419 cm^{-1} in the 3^{rd} recycled trunk catalyst are due to the C–O stretching and bending vibrations indicating the metal carbonate in the form of K_2CO_3. These results are in good agreement with the FT-IR results which were shown due to the metal carbonates present in the agro-waste catalysts reported by Rajkumari and Rokhum (2020), and Jitjamnong et al. (2020). The bands at 1123 and 1124 cm^{-1} may be attributed to K–O bond vibrations (Fan et al.,

2019). The peaks observed at 1013, 1080, 1058 and 1016 cm^{-1} are due to the vibrations of Si–O–Si bond of SiO_2 present in the catalysts. These data are in agreement with the FT-IR peaks of catalysts derived from plantain fruit peels (Etim et al., 2018), *Brassica nigra* (Nath et al., 2019), and rice husk (Zhao et al., 2018). The weak peaks at 668, 694, 704, 867, 864, 869 and 866 cm^{-1} may be due to stretching vibrations of metal–O bonds. The FT-IR spectral analyses of the present study are according to the predicted results of powder XRD patterns (**Fig. 2.2**) which confirmed the presence of metal carbonates and various metal oxides in the *M. paradisiaca* catalysts.

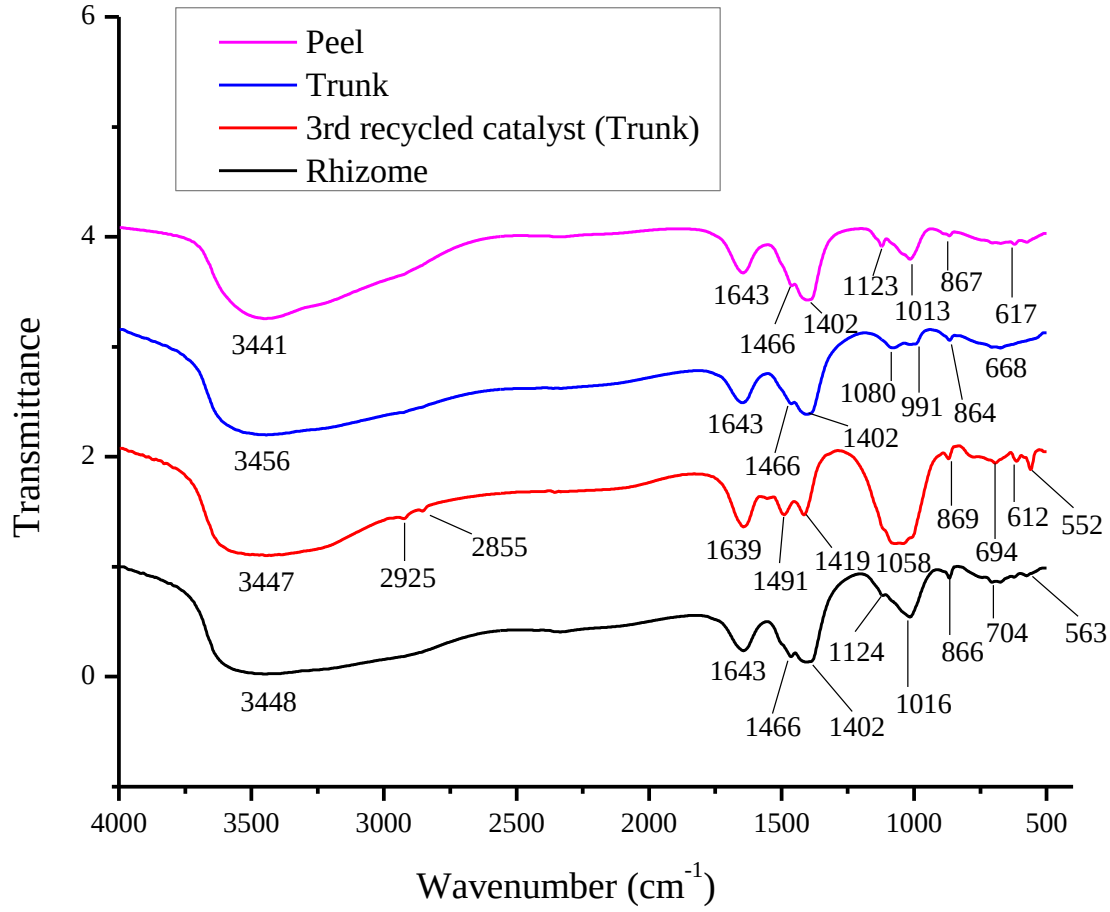

Fig. 2.3. FT-IR spectra of calcined *M. paradisiaca* catalysts.

2.3.1.3 BET analysis

The surface area and porosity of the catalyst play an influential role in the activity of the heterogeneous base catalyst (Balajii and Niju, 2019). In this study, the BET surface area of the calcined *M. paradisiaca* peel, trunk, and rhizome catalysts were found to be 4.1, 6.4 and 7.0 $m^2 g^{-1}$ (**Table 2.1**), and accordingly, the Barrett-Joyner-Halenda (BJH) pore volumes were found to be 0.01, 0.014 and 0.006 $cm^3 g^{-1}$. The pore size distributions of the catalysts (**Fig. 2.4**) were found to be ranging from 0.8–11.2 nm for peel, 1.7–7.4 nm for the trunk and 0.1–17.7 nm for rhizome along with the average pore diameters of 2.1, 2.6 and 2.1 nm (**Table 2.1**), which are uniform and expressive of borderline micro-mesoporous structure. Gor et al. (2012) reported the characterization of material with micro-mesoporous structure. Similar types of isotherms to that of the present catalysts (**Fig. 2.4**) were also reported for micro-mesoporous structured zeolites (Ordomsky et al., 2007; Thommes, 2010). Mesoporous catalyst-assisted biodiesel synthesis reactions have been reported with good catalytic properties (**Table 2.1**) and this is due to their ability to accommodate the basic active sites that enhance the catalytic activity (Rajkumari and Rokhum, 2020). The satisfactory yield of biodiesel is also due to the large BET surface area of the catalyst (Changmai et al., 2020a). The catalysts prepared from different waste biomasses (**Table 2.1**) with low surface areas have been reported in biodiesel synthesis with good catalytic properties. The low surface area of the catalyst might be due to the agglomeration of the particles after the calcination at high temperatures (Miladinović et al., 2020). The presence of a small quantity of unburnt carbon-particles in the ash sample may also be the reason for the low surface area of the catalyst, and the higher unburnt carbon-particles due to their porous structures contribute to a larger surface area (Pathak et al., 2018). Though the present *M. paradisiaca* catalysts are exhibiting low surface areas, the catalytic activities were found to be highly satisfactory with excellent biodiesel yields. This is due to the highly basic nature of the material that arises because of the dominant quantity of alkali and alkaline earth metal carbonates and oxides (**Table 2.2**, **Fig. 2.2**) that facilitate the strong basic sites on the surface of the catalyst to carry out the reaction (Rajkumari and Rokhum, 2020).

Table 2.1: Physical properties of agro-wastes derived ash-based catalysts utilized in biodiesel production.

Ash catalyst	**Surface area ($m^2 g^{-1}$)**	**Pore diameter (nm)**	**Pore volume ($cm^3 g^{-1}$)**	**Type of isotherm**	**Porous type**	**References**
M. paradisiaca peel	4.1	2.1	0.010	Type IV	Micro-mesoporous	This work
M. paradisiaca trunk	6.4	2.6	0.014	Type IV	Micro-mesoporous	This work
M. paradisiaca rhizome	7.0	2.1	0.006	Type IV	Micro-mesoporous	This work
M. acuminata peel	1.4	14.1	0.005	Type IV	Mesoporous	Pathak et al. (2018)
Sesamum indicum	3.6	1.6	0.012	Type IV	Mesoporous	Nath et al. (2020)
Brassica nigra	7.3	1.6	0.011	Type I	Microporous	Nath et al. (2019)
M. balbisiana underground stem	38.7	0.2	0.042	-	-	Sarma et al. (2014)
Lemna perpusilla	9.6	4.5	0.0217	-	-	Chouhan and Sarma (2013)
M. balbisiana peel	14.0	2.6	0.074	-	-	Gohain et al. (2017)
Walnut shell	8.8	-	-	-	-	Miladinović et al. (2020)
Banana peel	4.4	17.8	0.020	-	-	Betiku et al. (2016)
M. balbisiana trunk	1.4	-	-	-	-	Deka and Basumatary (2011)
Tucumã peel	1.0	-	-	-	-	Mendonça et al. (2019b)

Carica papaya stem	78.6	1.6	0.349	Type IV	Mesoporous	Gohain et al. (2020a)
M. sapientum peel	36.7	12.2	0.085	-	-	Jitjamnong et al. (2020)
Orange peel	605.6	2.8	0.428	Type IV	Mesoporous	Changmai et al. (2020a)
Banana trunk	39.0	2.7	0.21	Type IV	Mesoporous	Rajkumari and Rokhum (2020)
M. acuminata peduncle	45.9	9.7	0.14	-	-	Balajii and Niju (2019)

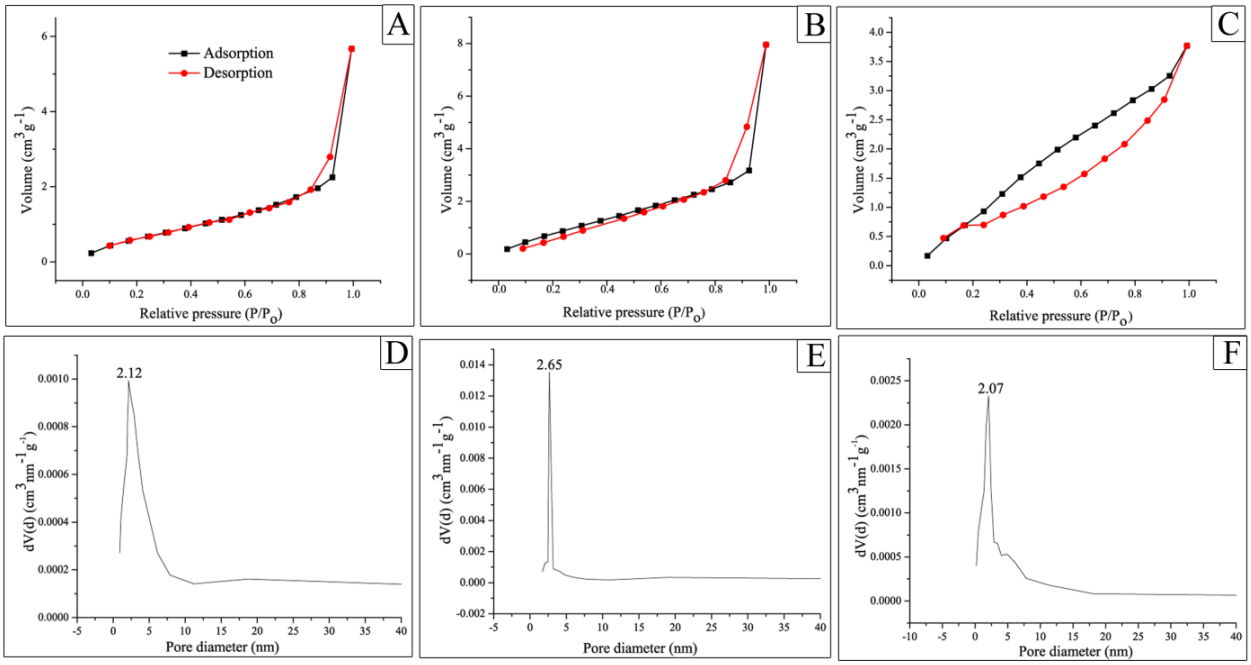

Fig. 2.4. N_2 adsorption-desorption isotherm (A–C) and adsorption pore size distribution (D–F) of *M. paradisiaca* peel (A, D), trunk (B, E) and rhizome (C, F) catalysts.

2.3.1.4 FESEM analysis

The surface morphology of the *M. paradisiaca* catalysts, and the 3rd recycled catalyst was studied from the FESEM images shown in **Fig. 2.5** (A, C, E) and **Fig. 2.6** (A–C). The images exhibited the morphological differences of the catalysts with the number of aggregates of porous materials and the spongy, sheet, or plate-like nature of materials. These types of morphologies are in support of the characters of porosity of the materials. The images of peel and rhizome catalysts **Fig. 2.5 (**A, E) showed the smooth and flat nature of the particles with comparatively less spongy than the trunk catalyst (**Fig. 2.5** C). The agglomerated particles were observed to be more in the trunk catalyst (**Fig. 2.5** C) compared to the catalysts of peel (**Fig. 2.5** A) and rhizome (**Fig. 2.5** E). This study also showed more porosity in the trunk catalyst (**Fig. 2.5** C) compared to peel and rhizome catalysts. The trunk catalyst exhibited better catalytic activity as the highly porous catalyst achieves higher efficiency in the processes of heterogeneous catalysis (Gohain et al., 2020a). The bright particles that appeared in the catalysts may be due to oxides or carbonates of potassium or other metals in the catalysts (Nath et al., 2019). Accordingly, the trunk catalyst (**Fig. 2.5** C) with more bright particles possessing more potassium concentration (**Fig. 2.5** D, **Table 2.2**) in the form of K_2CO_3 and K_2O (**Fig. 2.2**) showed higher catalytic activity compared to the peel and rhizome catalysts. The FESEM images of the burnt materials are shown in **Fig. 2.7** and representing the particles of non-uniform size and shape along with aggregates of particles and porous character of materials.

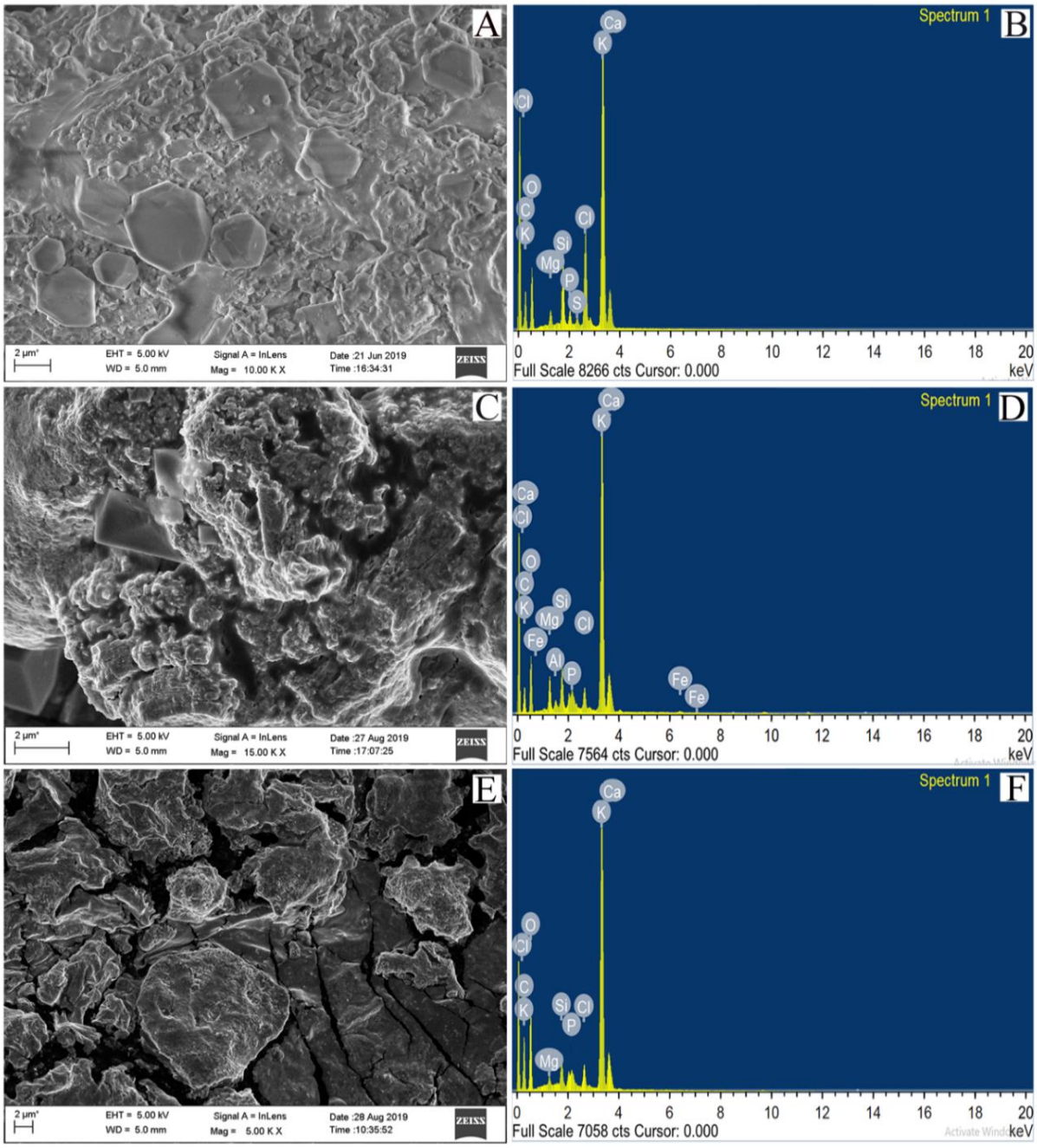

Fig. 2.5. FESEM images (A, C, E) and EDX spectra (B, D, F) of calcined *M. paradisiaca* peel (A, B), trunk (C, D) and rhizome (E, F) catalysts.

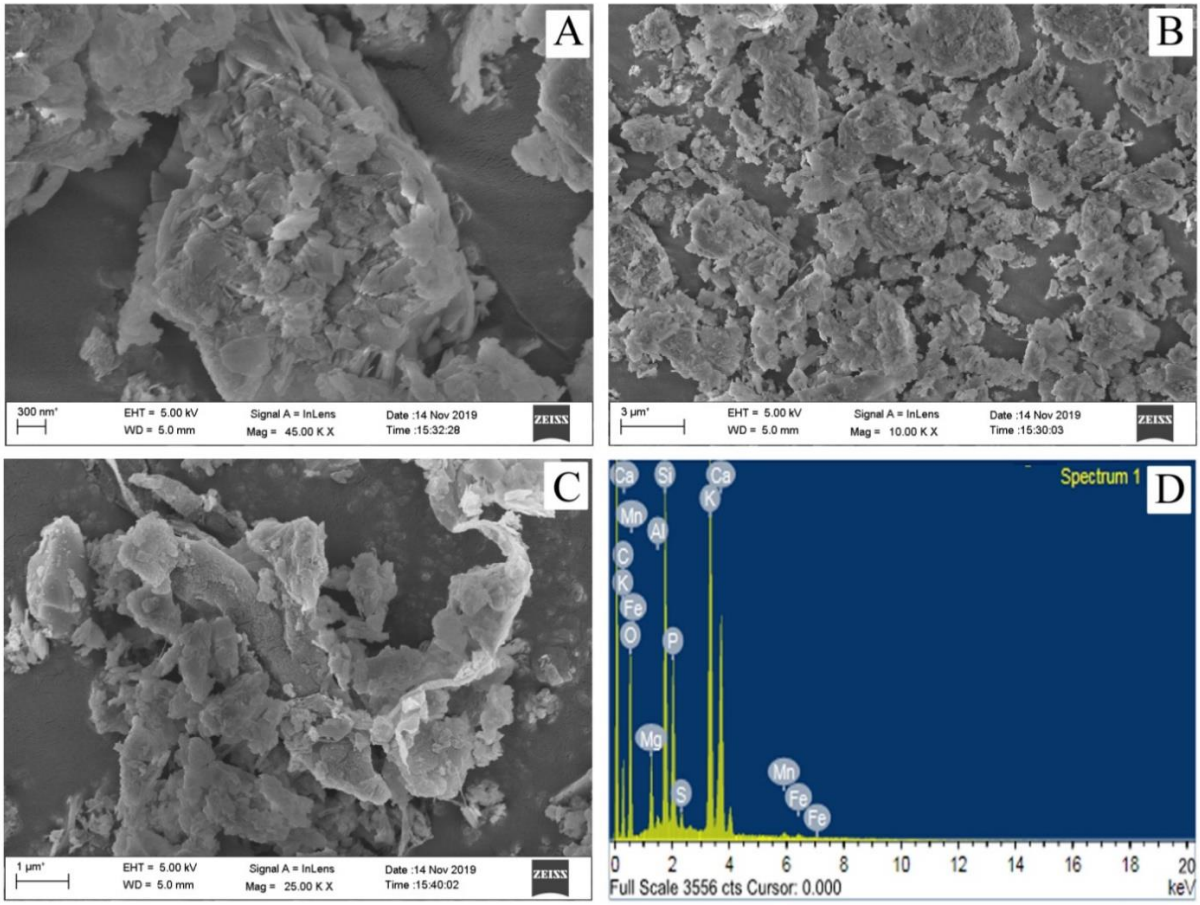

Fig. 2.6. FESEM images (A–C) and EDX spectrum (D) of 3rd recycled catalyst of *M. paradisiaca* trunk.

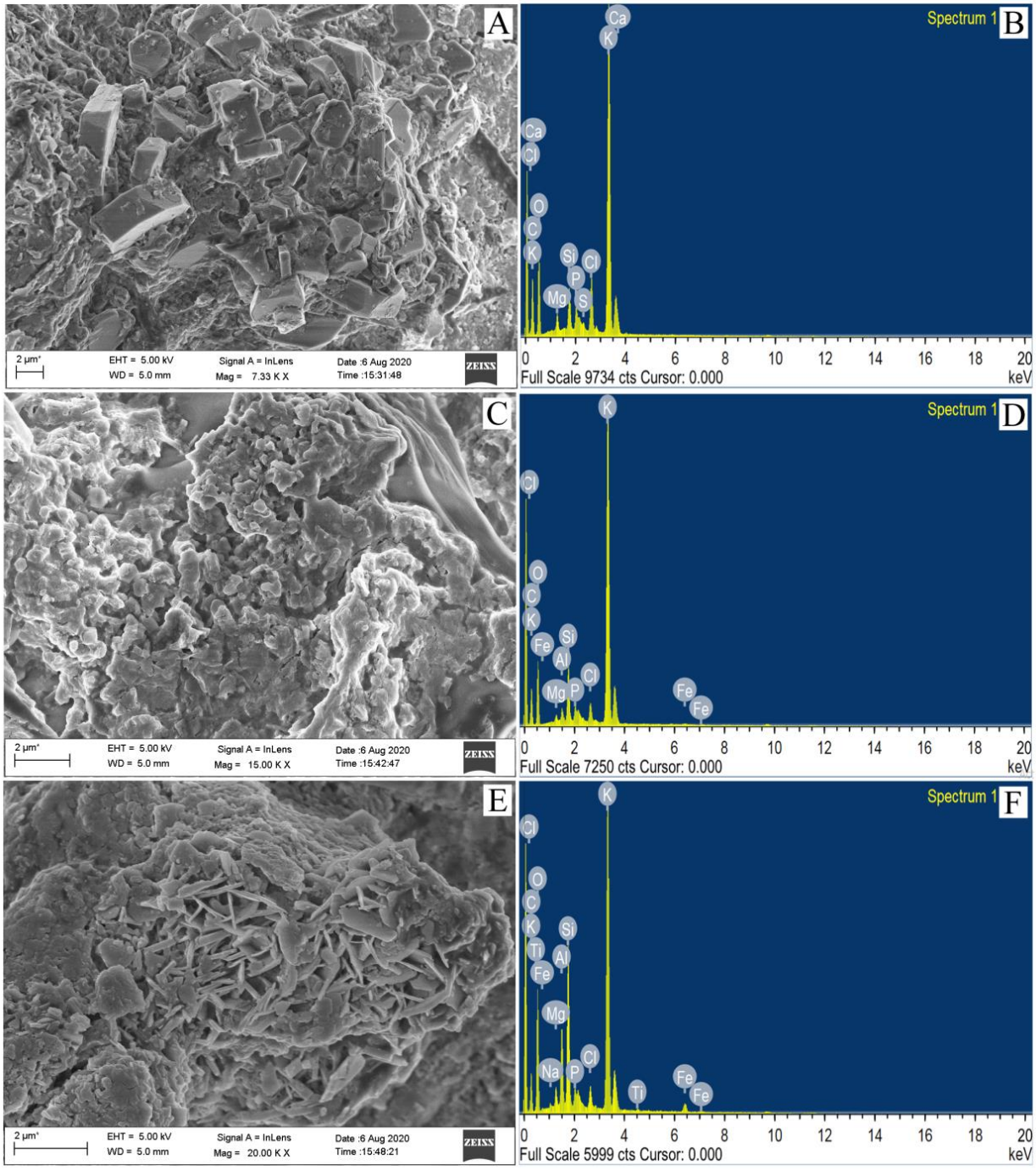

Fig. 2.7. FESEM images (A, C, E) and EDX spectra (B, D, F) of burnt materials of *M. paradisiaca* peel (A, B), trunk (C, D) and rhizome (E, F) catalysts.

2.3.1.5 Elemental composition of the catalyst

The elemental compositions of the *M. paradisiaca* catalysts and the 3rd recycled catalyst were studied using the EDX technique and depicted in **Fig. 2.5** (B, D, F) and **Fig. 2.6** D. The results are summarized in **Table 2.2**. The trunk catalyst with the highest amount of potassium (36.31 wt. %) compared to the rhizome catalyst (30.06 wt. %) and peel catalyst (29.25 wt. %) showed better activity in the reaction of *J. curcas* oil. It was reported that a higher percentage of the alkaline element in the agricultural waste-derived ash catalyst contributes better catalytic activity in biodiesel synthesis (Mendonça et al., 2019b). In this study, potassium was the dominant alkaline element (**Table 2.2**) present in the form of K_2CO_3 and K_2O which were supported by both XRD (**Fig. 2.2**) and FT-IR (**Fig. 2.3**) studies. Nath et al. (2019; 2020) studied the catalytic activities of *Brassica nigra* and *Sesamum indicum* catalysts in the production of biodiesel and reported that the catalyst with a high percentage of potassium signifies good catalytic activity. Betiku et al. (2017), and Balajii and Niju (2019) also reported that a high concentration of potassium in the catalyst plays a major role in terms of conversion and activity. A summary of the composition of the catalysts derived from different waste biomasses is shown in **Table 2.3**. *M. paradisiaca* trunk catalyst exhibited better catalytic activity compared to *Sesamum indicum* (Nath et al., 2020), *Lemna perpusilla* (Chouhan and Sarma, 2013), *Acacia nilotica* (Sharma et al., 2012), *Musa balbisiana* rhizome (Sarma et al., 2014), camphor tree leaf (Li et al., 2018), *Brassica nigra* (Nath et al., 2019), *Musa balbisiana* peel (Gohain et al., 2017) and *Carica papaya* stem (Gohain et al., 2020a) catalysts. This may be due to the presence of higher potassium amount in the form of K_2CO_3 as the active component in the *M. paradisiaca* trunk catalyst than these reported catalysts. It is observed from **Table 2.3** that most of the researchers did not report the percentages of carbon and oxygen in their catalysts (Gohain et al., 2017; Nath et al., 2019; Gohain et al., 2020a), and for that reason, the percentage of potassium in their catalysts appeared higher which might decrease if the carbon and oxygen contents are reported. Balajii and Niju (2019; 2020) also have not reported carbon contents in their catalysts for which their potassium contents appeared high and the catalysts exhibited comparable catalytic activities. In this study, the *M. paradisiaca* trunk catalyst with 36.31 wt. % of potassium in the form of carbonate (**Fig. 2.2**, **Fig. 2.3**) as the active component contributed excellent activity in biodiesel synthesis. The detailed elemental compositions of the burnt materials identified using the FESEM-EDX technique are presented in **Table 2.4**. This analysis showed that the calcined catalysts (**Table 2.2**) contained more K concentration than that of the burnt materials (**Table 2.4**), and K was found to play a major role in catalysis.

Table 2.2: FESEM-EDX analyses of calcined *M. paradisiaca* catalyst.

Elements	**Composition of catalyst calcined at 550 ºC**							
	***M. paradisiaca* peel**		**Trunk**		**3rd recycled catalyst (Trunk)**		**Rhizome**	
	Weight %	**Atomic %**	**Weight %**	**Atomic %**	**Weight %**	**Atomic %**	**Weight %**	**Atomic %**
C	24.02	38.04	13.22	22.88	20.57	32.09	18.43	29.54
O	33.34	39.64	37.87	49.23	39.20	45.92	43.27	52.06
K	29.25	14.23	36.31	19.31	13.79	6.61	30.06	14.80
Ca	4.01	1.70	2.21	1.14	9.44	4.42	3.06	0.30
Mg	1.08	0.85	3.08	2.63	2.11	1.63	0.69	0.55
Si	3.81	2.58	2.84	2.11	8.12	5.41	1.67	1.14
P	1.06	0.65	1.12	0.75	5.30	3.20	1.00	0.62
S	0.43	0.25	–	–	0.53	0.31	–	–
Cl	3.01	2.07	2.13	1.24	–	–	1.83	1.00
Al	–	–	0.63	0.48	0.26	0.18	–	–
Fe	–	–	0.59	0.22	0.30	0.10	–	–

Table 2.3: Elemental composition of various agro-wastes derived ash-based catalysts.

Ash catalyst	Calcination conditions	Composition (%)													
		Na	**K**	**Ca**	**Mg**	**Al**	**Si**	**P**	**Cl**	**Fe**	**Mn**	**Zn**	**Sr**	**C**	**O**
M. paradisiaca trunk (This work)	550 ^{o}C, 2 h	–	36.31	2.21	3.08	0.63	2.84	1.12	2.13	0.59	–	–	–	13.22	37.87
Brassica nigra (Nath et al., 2019)	550 ^{o}C, 2 h	0.94	56.13	26.04	2.86	–	5.37	–	–	1.26	0.05	1.63	5.72	–	–
Sesamum indicum (Nath et al., 2020)	550 ^{o}C, 2 h	1.42	29.64	33.80	9.68	–	11.32	–	–	1.70	0.80	0.54	11.09	–	–
Lemna perpusilla (Chouhan and Sarma, 2013)	550 ^{o}C, 2 h	0.53	11.32	–	–	–	82.51	–	–	–	–	–	–	5.10	–

Musa balbisiana underground stem (Sarma et al., 2014)	550 °C, 2 h	0.61 (Na_2O)	25.09 (K_2O)	10.44 (CaO)	10.04 (MgO)	4.07 (Al_2O_3)	35.92 (SiO_2)	4.47 (P_2O_5)	–	1.88 (Fe_2O_3)	–	–	1.89 (SrO)	–	–
Acacia nilotica tree stem (Sharma et al., 2012)	500 °C, 3 h	0.6	6.7	13.3	2.7	8.3	15.7	0.80	–	–	–	–	–	–	–
Musa paradisiacal peels (Etim et al., 2018)	700 °C, 4 h	–	51.02	–	1.15	0.29	2.51	1.84	6.27	–	–	–	–	–	36.43
Musa balbisiana peels (Gohain et al., 2017)	700 °C, 4 h	10.41	41.37	36.08	12.02	–	–	–	–	–	–	–	–	–	–
Carica papaya stem (Gohain et al., 2020a)	700 °C, 4 h	14.78	56.71	21.08	4.41	–	3.02	–	–	–	–	–	–	–	–

Musa acuminata peduncle (Balajii and Niju, 2019)	700 °C, 4 h	–	42.23	1.70	1.39	–	1.54	1.91	–	–	–	–	–	–	50.54
Musa acuminata peduncle (Balajii and Niju, 2019)	Uncalcined	–	25.63	–	0.97	–	0.56	0.78	–	–	–	–	–	–	72.06
Musa spp peduncle (Balajii and Niju, 2020)	700 °C, 4 h	–	52.04	5.27	5.71	–	–	–	–	–	–	–	–	–	36.99
Acacia nilotica tree stem (Sharma et al., 2012)	800 °C, 3 h	5.7	5.7	17.8	4.5	1.2	21.5	0.5	–	–	–	–	–	–	–
Camphor tree leaf (Li et al., 2018)	800 °C, 2 h	0.23	1.22	12.05	1.82	2.70	–	–	–	–	–	–	–	–	–

Table 2.4: FESEM-EDX analyses of *M. paradisiaca* burnt materials.

Elements	**Composition of *M. paradisiaca* burnt materials**					
	***M. paradisiaca* peel**		**Trunk**		**Rhizome**	
	Weight %	**Atomic %**	**Weight %**	**Atomic %**	**Weight %**	**Atomic %**
C	25.89	38.93	17.67	28.82	17.49	27.70
O	38.71	43.71	39.60	48.49	42.20	50.16
K	25.93	11.98	34.48	17.28	23.40	11.38
Ca	1.32	0.59	–	–	–	–
Na	–	–	–	–	0.30	0.24
Mg	1.07	0.79	0.56	0.45	1.06	0.83
Si	2.11	1.36	3.97	2.77	7.75	5.25
P	1.12	0.65	0.82	0.52	0.71	0.44
S	0.23	0.13	–	–	–	–
Cl	3.62	1.84	1.78	0.98	1.36	0.73
Al	–	–	0.78	0.57	3.61	2.54
Fe	–	–	0.35	0.12	1.90	0.65
Ti	–	–	–	–	0.24	0.09

XPS technique was employed to investigate the surface compositions of the catalysts (**Fig. 2.8**, **Table 2.5**). In the XPS technique too, potassium was identified as the predominant one among the various metals present with the highest percentage being in the *M. paradisiaca* trunk catalyst (20.32 %) followed by rhizome catalyst (15.50 %) and peel catalyst (14.15 %). This is strongly in agreement with the reports of FESEM-EDX studies (**Table 2.2**). The potassium in the *M. paradisiaca* catalysts was present as K_2CO_3, K_2O and KCl which were supported by powder XRD (**Fig. 2.2**) and FT-IR (**Fig. 2.3**) results. The high-resolution O 1s XPS spectra (**Fig. 2.8** B) of *M. paradisiaca* peel, trunk and rhizome catalysts showed a peak at 530.50 eV demonstrating the binding energies of oxygen element present as oxides in the catalysts (Nath et al., 2019). In the XPS spectra of C 1s (**Fig. 2.8** C), the two peaks at 284.78 and 288.48 eV (peel), 284.88 and 288.6 eV (trunk), and 284.87 and 288.57 eV (rhizome) are exhibiting the binding energies of sp^2 carbon (C=O) of the carbonates of the metal present in the catalysts (Pathak et al., 2018). The potassium present in catalysts in the form of carbonate or oxide displayed the XPS peaks (**Fig. 2.8** D) at binding energies of 292.5 and 295.3 eV (Nath et al.,

2020). The high-resolution spectra of Ca 2p (**Fig. 2.8** E) represented two peaks for peel, trunk and rhizome catalysts with binding energies of 346.4 and 350.3 eV which may be due to the oxide or carbonate of calcium (Zhao et al., 2018). The oxide of silicon present in the catalysts indicated a single peak (**Fig. 2.8** F) with the binding energy of 101.8 eV for both trunk and rhizome catalysts. The peel catalyst showed a peak at 102.2 eV for the oxide of silicon (SiO_2). The results are in agreement with the XRD analysis (**Fig. 2.2**). It was found from XPS studies (**Table 2.5**) that C, O and K were the three major components that existed as K_2CO_3 (**Fig. 2.2**, **Fig. 2.3**), and the C (50.75 %) and K (20.32 %) were found to be the highest in the *M. paradisiaca* trunk catalyst compared to the other two catalysts.

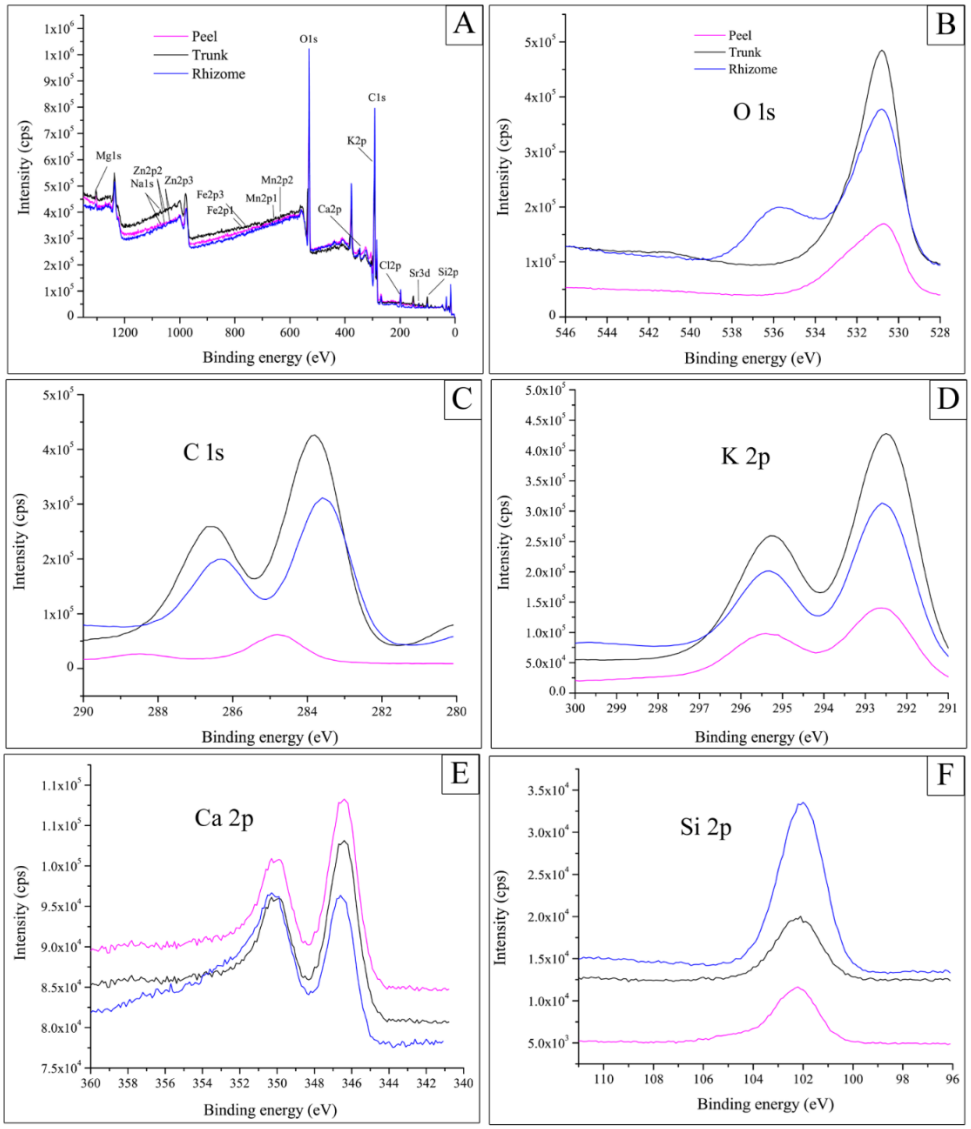

Fig. 2.8. XPS survey spectra (A) of *M. paradisiaca* peel, trunk and rhizome catalysts calcined at 550 ^{o}C; XPS spectra of O 1s (B), C 1s (C), K 2p (D), Ca 2p (E) and Si 2p (F).

Table 2.5: XPS analyses of *M. paradisiaca* catalysts calcined at 550 ºC.

Elements	Composition (Atomic %)		
	***M. paradisiaca* peel**	**Trunk**	**Rhizome**
C1s	48.92	50.75	37.29
O1s	29.25	19.43	27.74
K2p	14.15	20.32	15.50
Si2p	3.50	5.69	16.2
Cl2p	2.38	2.09	0.88
Mg1s	0.60	0.13	0.59
Ca2p	0.34	0.21	0.29
Na1s	0.27	0.06	0.28
Fe2p	0.26	0.26	0.30
Mn2p	0.23	0.31	0.34
Sr3d	0.10	0.54	0.26
Zn2p	–	0.21	0.33

2.3.1.6 HRTEM analysis

The *M. paradisiaca* catalysts were analyzed to know the structural information using HRTEM and the results are shown in **Fig. 2.9**. The images of the catalysts depicted in **Fig. 2.9** (A, E, I) are showing the clustered particles of irregular size and shape. Some nano-structures with few spherical shaped particles along with different shaped structures are observed from the images shown in **Fig. 2.9** (B, C, F, G, J, K). The catalysts from the peel (**Fig. 2.9** C), trunk (**Fig. 2.9** G) and rhizome (**Fig. 2.9** K) showed fringes like topology which is one of the foremost characters for the porous materials. Polycrystalline natures of the *M. paradisiaca* catalysts are revealed from SAED patterns shown in **Fig. 2.9** (D, H, L). Polycrystalline nature of the materials derived from *Brassica nigra*, *Sesamum indicum* and *Eichhornia crassipes* plants were successfully reported as the base heterogeneous catalysts by Nath et al. (2019; 2020) and Talukdar and Deka (2016). It has been reported that the catalysts with smaller clusters of nano-sized particles possess efficient activity for the reaction (Aslam et al., 2014; Nath et al., 2019). BET, FESEM and HRTEM techniques indicated that the present *M. paradisiaca* catalysts consisted of characters of porous materials and the polycrystalline nano-structured particles which exhibited high efficiency in the catalytic activity of biodiesel conversion via transesterification.

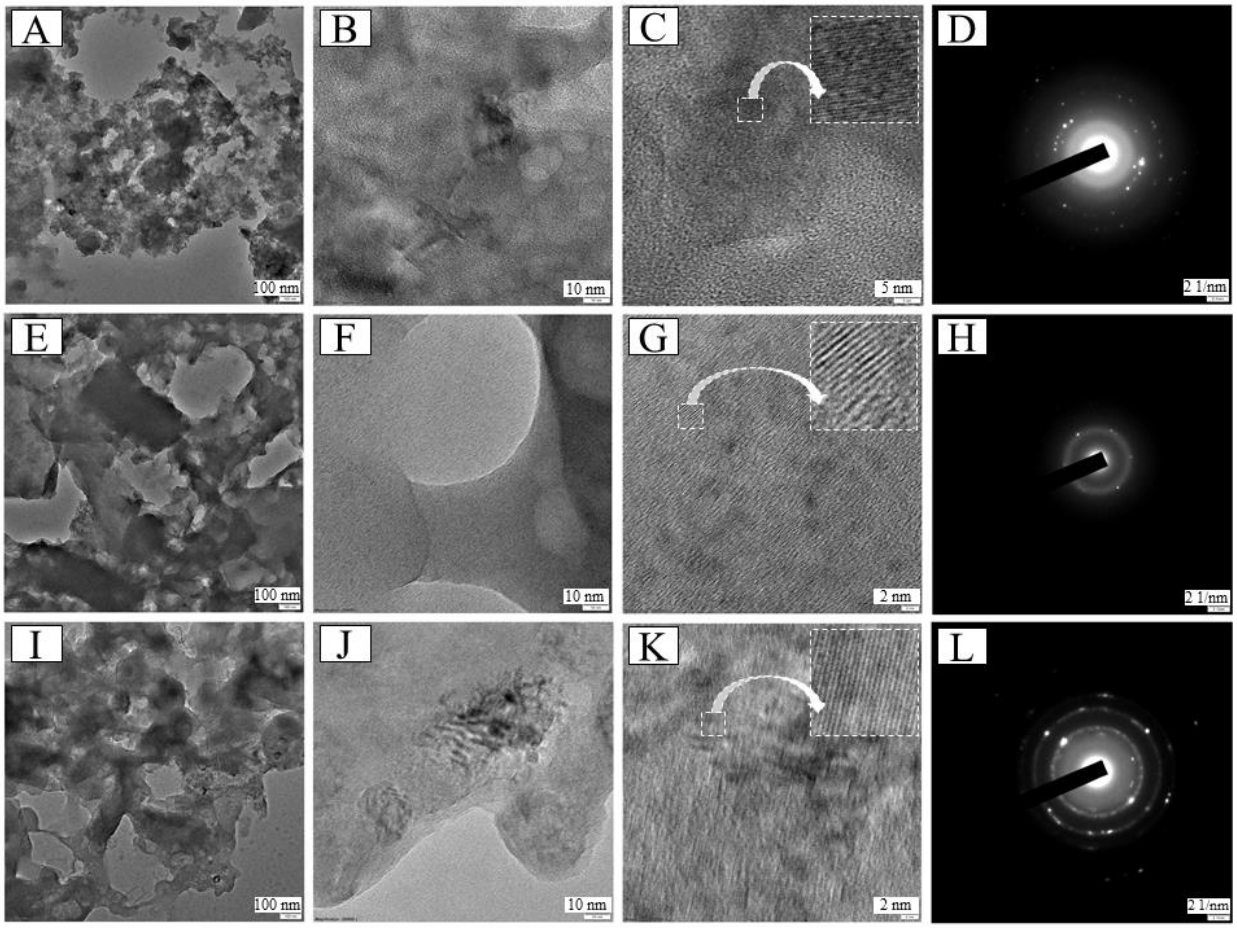

Fig. 2.9. TEM images and SAED patterns (D, H, L) of *M. paradisiaca* peel (A–D), trunk (E–H) and rhizome (I–L) catalysts.

2.3.1.7 Determination of pH value of the catalysts

The pH values of the calcined *M. paradisiaca* peel, trunk, and rhizome catalysts are represented in **Fig. 2.10**. The high pH values of the solutions were observed in the ratio of 1:5 w/v, and the pH values decrease slightly at 1:40 w/v. The aqueous solutions with high pH obtained from the dissolution of ash samples not only correspond to the basic character of the solid sample but also indicates their instability in aqueous solution. If the aqueous solutions are less basic, it possibly signifies the results from the variation in samples' stability. Among the three *M. paradisiaca* catalysts, the trunk (stem) catalyst was found to be a stronger base with a higher pH value, and this may be due to the presence of the higher amount of potassium that was revealed from the studies of FESEM-EDX (**Table 2.2**) and XPS (**Table 2.5**). As a result, the excellent activity of the catalyst in terms of reaction rate and product yield was achieved for the present jatropha biodiesel synthesis. It has been reported that the high pH value of the material is due to the presence of a high percentage of alkali metals particularly potassium in

the catalyst (Nath et al., 2019). Nath et al. (2019; 2020) utilized *Brassica nigra* and *Sesamum indicum* catalysts in biodiesel production and their reported pH values at 1:20 w/v were 11.76 and 11.30, and the catalytic activities of these catalysts in biodiesel synthesis were found to be inferior compared to the present *M. paradisiaca* catalysts. Reasonably a low pH value of 9.6 (1:20 w/v) for *Eichhornia crassipes* ash catalyst was also reported by Talukdar and Deka (2016).

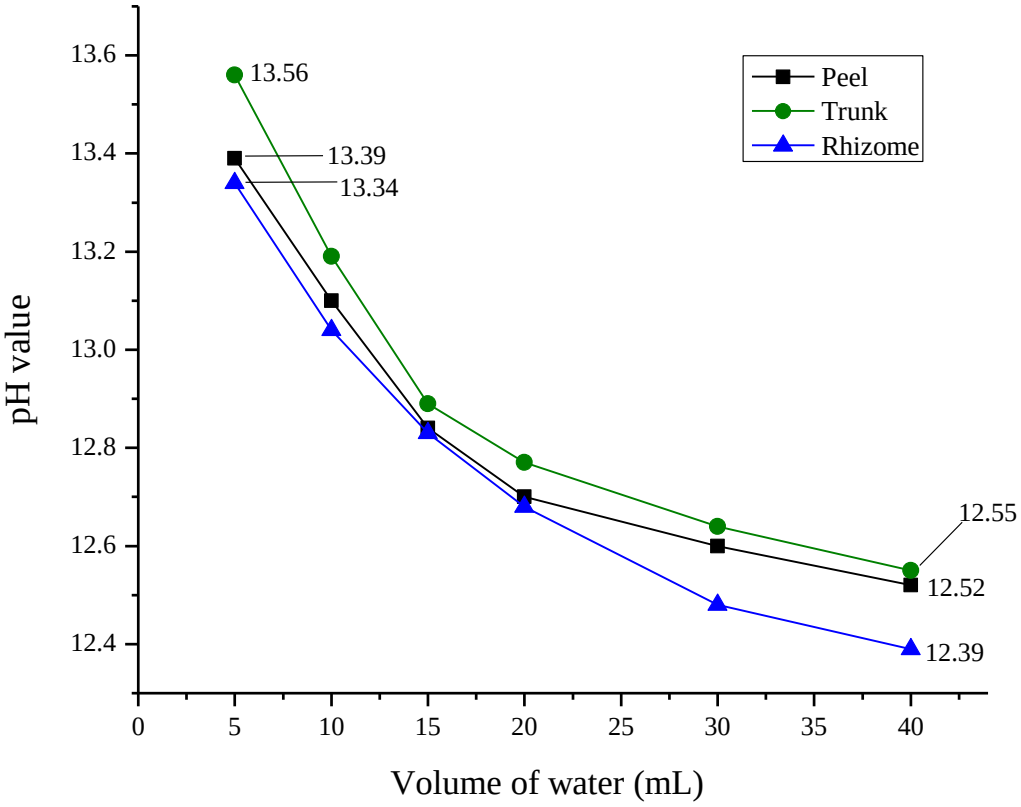

Fig. 2.10. pH value variation of calcined *M. paradisiaca* peel, trunk and rhizome catalysts (1 g) with different volume of water.

The elemental analysis (Na, K, Ca, Fe, Mn, P and Cl) of the liquid samples of the *M. paradisiaca* catalysts at 1:5 w/v was carried out to know the concentration of the elements in the solution, and the results are shown in **Table 2.6**. In the analysis, K was found to be the predominant element followed by Cl in all the three liquid samples of *M. paradisiaca* catalysts (peel, trunk and rhizome). The concentration of K in the catalyst solution at 1:5 w/v was found in the increasing order of 41225.0 mg/L (rhizome) < 42788.6 mg/L (peel) < 56730.0 mg/L (trunk), and at the same ratio, pH value was also found in a similar order (**Fig. 2.10**), indicating

highly alkaline solution. The highest K concentration detected in the solution of *M. paradisiaca* trunk catalyst is in well-agreement with the results depicted by EDX and XPS studies.

Table 2.6: Elemental analysis of liquid samples of the catalysts at 1:5 w/v.

Elements	Elemental composition (mg/L)		
	***M. paradisiaca* peel (1:5 w/v)**	**Trunk (1:5 w/v)**	**Rhizome (1:5 w/v)**
Na	67.56	82.75	288.0
K	42788.6	56730.0	41225.0
Ca	25.50	17.67	12.59
Fe	0.30	0.34	0.68
Mn	0.06	0.05	0.39
P	211.89	179.05	189.0
Cl	8450.80	8786.25	5112.0

2.3.1.8 Soluble alkalinity of catalyst

The soluble alkalinity was estimated and found to be 4.03, 5.10 and 5.43 mmol g^{-1} for *M. paradisiaca* peel, rhizome and trunk catalysts. Mendonça et al. (2019b) tested the alkalinity of tucumã peel catalyst calcined at 800 °C, and 3.7 mmol g^{-1} of soluble alkalinity was reported. A low soluble alkalinity value of 1.05 mmol g^{-1} was reported for cupuaçu catalyst calcined at 800 °C (Mendonça et al., 2019a). The higher soluble alkalinity found in the *M. paradisiaca* catalysts is possibly linked to the presence of a higher concentration of components like carbonates and/or phosphates of alkali and alkaline earth metals (Mendonça et al., 2019a; 2019b). In this study, alkaline compound K_2CO_3 was characterized by XRD (**Fig. 2.2**) and FTIR (**Fig. 2.3**) studies, and phosphorus (P) was detected both in FESEM-EDX (**Table 2.2**, **Table 2.4**) and spectrophotometric (**Table 2.6**) techniques indicating the presence of metal phosphates. Sharma et al. (2012) reported higher soluble alkalinity of 12.7 mmol g^{-1} for the activated wood ash catalyst (800 ^oC) with 0.5 % mass fraction of K_2CO_3, which was due to an excess of K_2CO_3 present in the catalyst. They tested alkalinity in the methanol medium also and reported very low soluble alkalinity which was less than 0.1 mmol g^{-1}. In this study, as the transesterification reaction was performed using methanol, the soluble alkalinity was also tested in methanol medium following the same procedure. It is to be noted that lower soluble alkalinity values of 1.18, 1.66 and 1.71 mmol g^{-1} were obtained for *M. paradisiaca* peel, rhizome and trunk catalysts in the methanol solvent compared to that of the aqueous solution.

This may be due to the less polarity of methanol compared to the highly polar water molecule. Some inorganic components like metal carbonates and phosphates present in the *M. paradisiaca* catalysts are expected to be less soluble in methanol than water.

2.3.1.9 Basicity of catalyst

The assessment of basic strength of *M. paradisiaca* catalysts using Hammett indicator displayed that all the three catalysts got a change in their color with bromothymol blue (H_ = 7.2), phenolphthalein (H_ = 9.3) and nile blue (H_ = 10.1). There was no change in color with 4-nitroaniline (H_ = 18.4). The basic strength of catalyst can be represented as "stronger than the weakest indicator that shows a color change, but weaker than the strongest indicator that shows no change in color" (Wang et al., 2012). The basic strengths of the *M. paradisiaca* catalysts were found to be within the limit of 10.1 < H_ <18.4. The trunk catalyst was found to have the highest basicity of 1.59 mmol g^{-1} followed by the peel catalyst of 1.43 mmol g^{-1} and the catalyst derived from the rhizome showed the lowest basicity of 1.39 mmol g^{-1}. Remarkably, this trend is according to the pH values of the catalysts (**Fig. 2.10**). *M. paradisiaca* catalysts displayed the catalytic efficiencies in the reaction (**Table 2.7**) in accordance with the basicity results. The turnover frequency (TOF) indicating the effectiveness of catalyst is one of the major criteria to become an industrial or commercial catalyst, and it was determined based on the number of the molecule of the product obtained per unit basic site and per time (Roy et al., 2020b), and found to be 68.24, 56.85 and 46.16 min^{-1} for *M. paradisiaca* trunk, peel and rhizome catalysts.

2.3.2 Catalytic activity of the catalyst

2.3.2.1 Effect of catalyst loading

Catalyst loading with respect to the oil (triglyceride) plays a crucial role in the heterogeneous base-catalyzed transesterification of biodiesel synthesis (Nath et al., 2019). Investigation on the effect of catalyst concentration on the rate of transesterification reaction and yield of biodiesel with 9:1 MTOMR was carried out using different amounts of *M. paradisiaca* trunk catalyst at 65 ^{o}C and the results are presented in **Fig. 2.11**. On increasing a load of catalyst from 3 to 5 wt. %, the reaction time is significantly decreased with the increase of biodiesel yield (**Fig. 2.11**). It is remarkable that on increasing the catalyst load from 5 to 7 wt. % and then to 9 wt. %, no significant decrease in the duration of reaction along with no further increase in the product yield was noticed. Nath et al. (2019) and Gohain et al. (2017) also studied the optimum level of catalyst loading of the catalysts derived from agro-wastes

and they reported that an increase in the amount of catalyst increases the yield of jatropha biodiesel to only a certain concentration of catalyst, and beyond that level, the yield of the product does not increase or it remains unchanged. This may be due to starting the formation of a side-product or backward reaction. In this study, 5 wt. % of catalyst loading that could complete the reaction in a reasonable reaction time of 9 min at 65 ^{o}C with a relatively high biodiesel yield of 97.65 % is considered as the optimum catalyst amount for effective production of biodiesel. Aslam et al. (2014), Kumar et al. (2016) and Sarma et al. (2014) also reported 5 wt. % of catalyst loading as the optimum condition for their transesterification reactions.

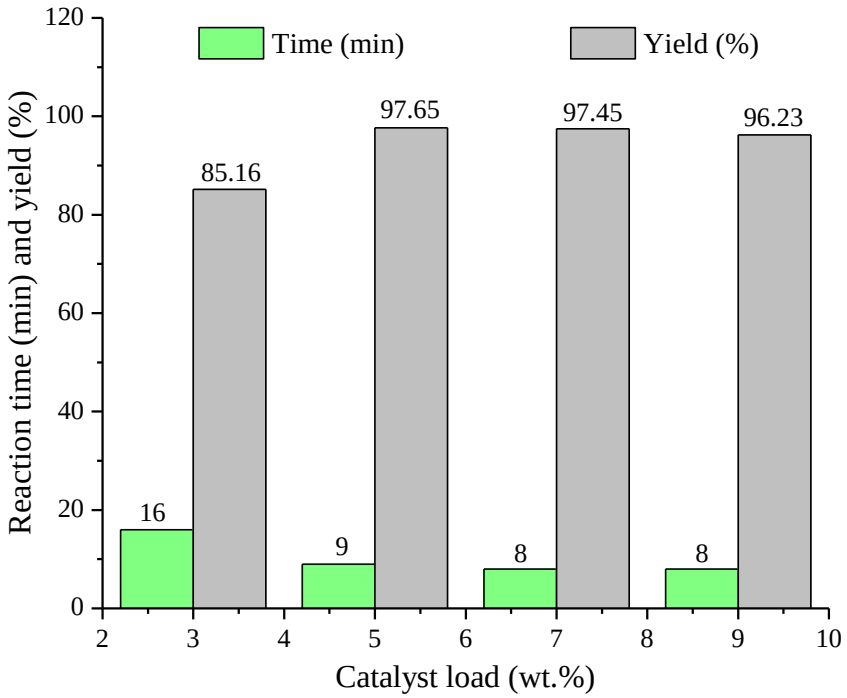

Fig. 2.11. Effect of *M. paradisiaca* trunk catalyst loading on biodiesel synthesis via transesterification reaction (Temperature = 65 ^{o}C, MTOMR = 9:1).

2.3.2.2 Effect of MTOMR

In this study, using the optimized catalyst loading of 5 wt. % of *M. paradisiaca* trunk, different MTOMR was applied in the reaction at 65 ^{o}C to determine the optimum level of MTOMR. The results obtained are shown in **Fig. 2.12**. It is depicted that the transesterification reaction time decreases on increasing the MTOMR from 3:1 to 9:1, and then it slightly increases beyond MTOMR of 12:1 up to 18:1. Accordingly, the yield of the biodiesel is increased from MTOMR of 3:1 to 9:1, and beyond 9:1 MTOMR, there is a gradual decrease in the biodiesel yield (**Fig.**

2.12). The decrease of biodiesel yield and increase of reaction time with increasing MTOMR beyond optimum level was also reported by Syazwani et al. (2015) and Nath et al. (2019; 2020). They stated that using a higher ratio of methanol resulted in the dilution of reaction mixtures and flooding of the active-sites of the catalyst, which then leads to a decrease of interactions. As a result, it increases the time period for completion of the reaction and the yield of the product decreases. Besides, exceeding the optimum level of MTOMR, there is a chance of the hydrolysis of produced alkyl esters (biodiesel) leading to the reduction of product yield due to the soap formation (Betiku et al., 2019). In this study, the biobased solid catalyst is utilized for biodiesel production (**Scheme 2.1**). Hydrolysis (saponification) of the produced biodiesel (**Scheme 2.2** and **2.3**) is rare with the solid catalyst or heterogeneous catalyst. Considering the facts, 9:1 MTOMR which could give a high yield of biodiesel with 5 wt. % of catalyst in a relatively lower reaction time at 65 ^{o}C is considered as the optimum ratio in this study. Similarly, 9:1 MTOMR was reported as the optimum ratio for biodiesel synthesis in the works of Aslam et al. (2014) and Kumar et al. (2016).

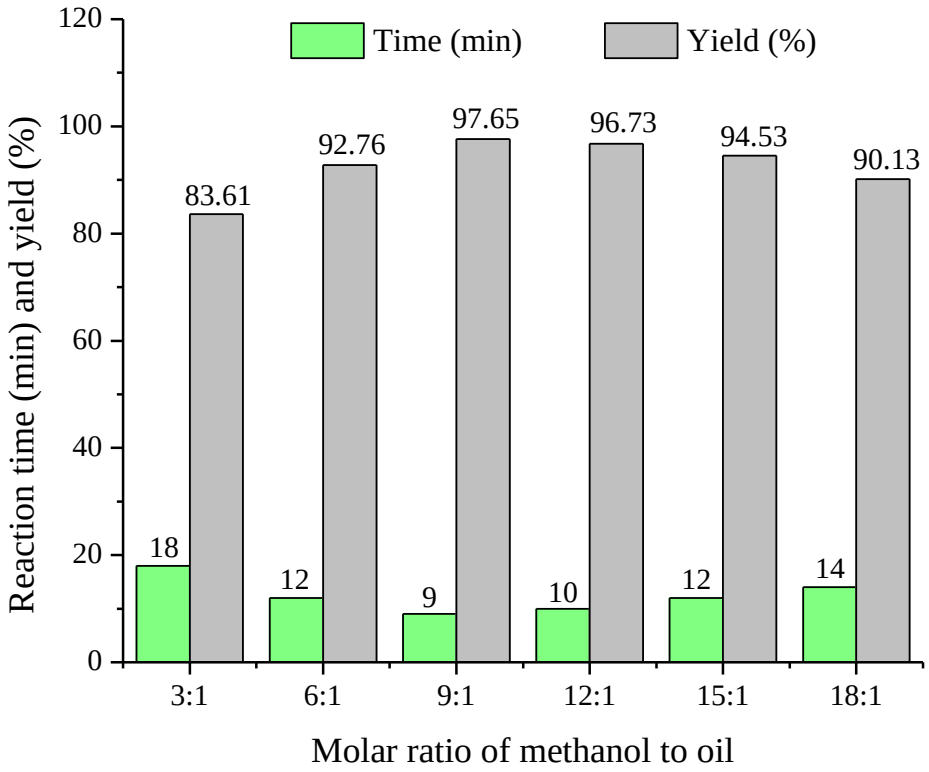

Fig. 2.12. Effect of MTOMR on biodiesel synthesis (Temperature = 65 ^{o}C, calcined *M. paradisiaca* trunk catalyst loading = 5 wt.%).

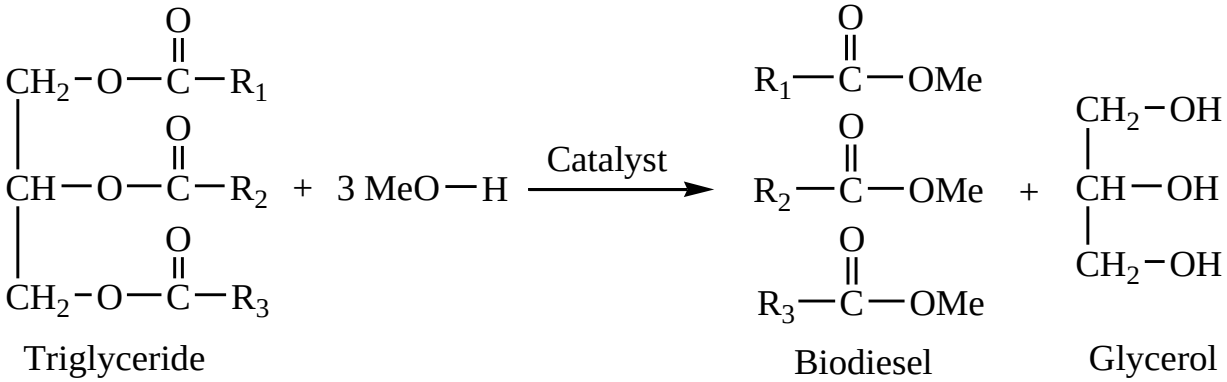

Scheme 2.1. Transesterification of triglyceride.

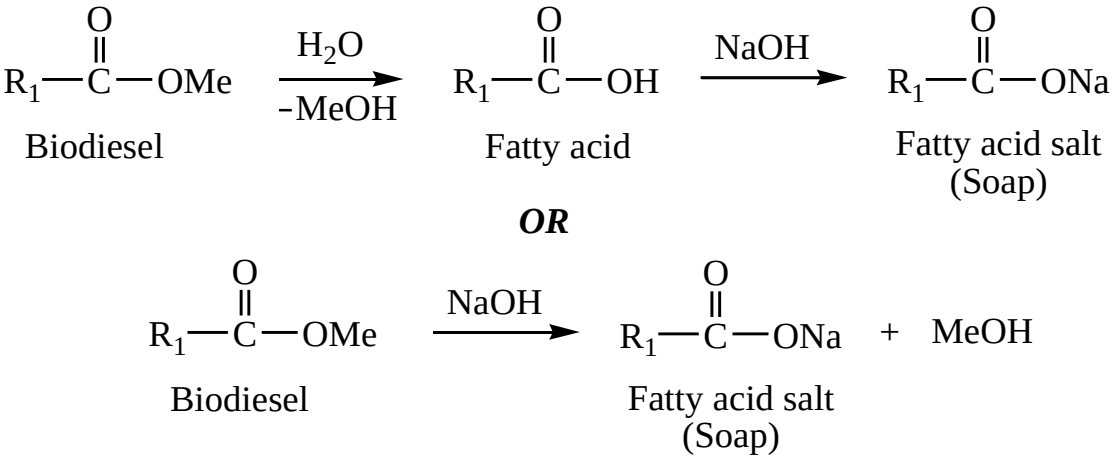

Scheme 2.2. Saponification reaction of biodiesel.

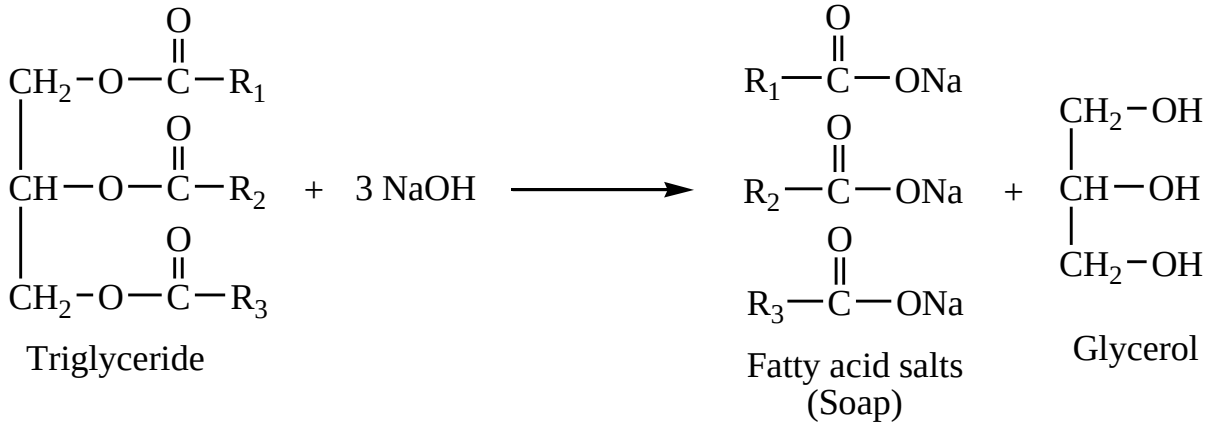

Scheme 2.3. Saponification of triglyceride.

2.3.2.3 Effect of temperature on the reaction

The temperature is one of the imperative factors which influence the transesterification rate for the production of biodiesel. To study the effect of temperature on transesterification, the reactions were carried out at different temperatures using the optimum reaction conditions (5 wt. % of *M. paradisiaca* catalysts and 9:1 MTOMR). The results are shown in **Fig. 2.13**. This demonstrated that there are significant decreases in reaction times with all the three catalysts used on increasing the temperature from 32 ^{o}C (room temperature) to 75 ^{o}C. No drastic changes or increase in the yields of biodiesel were noticed when the temperature was increased from 32 ^{o}C to 65 ^{o}C, and then to 75 ^{o}C (**Fig. 2.13**). Comparative studies using the three different *M. paradisiaca* catalysts showed that an increase of reaction temperature from 65 to 75 ^{o}C is not showing a significant decrease in reaction time along with the non-significant increase of biodiesel yield. Increasing the reaction temperature beyond 65 ^{o}C is not contributing to the transesterification for better catalytic activities. Further, the reaction at the higher temperature (beyond 65 ^{o}C) also needs additional precautions and leads to additional usage of energy which would increase the cost of produced biodiesel. Among the different investigated reaction temperatures, the trunk catalyst is showing better activity and satisfactory results at 65 ^{o}C in terms of both reaction time required for reaction completion and biodiesel yield. The reaction temperature of 65 ^{o}C is considered as the optimum for the effective production of biodiesel in the current study.

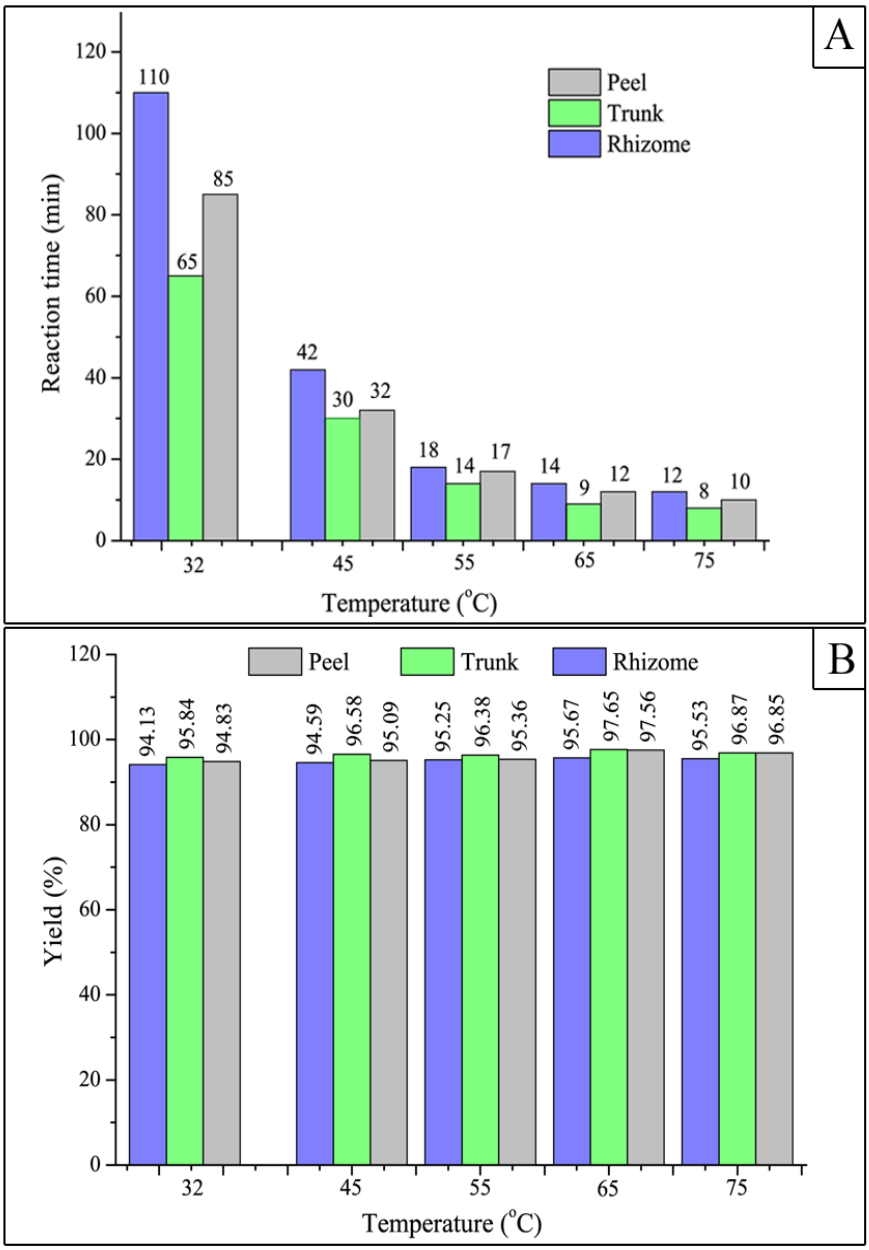

Fig. 2.13. Effect of temperature on biodiesel synthesis. Reaction conditions: MTOMR = 9:1, catalyst loading (*M. paradisiaca* peel, trunk and rhizome) = 5 wt.%.

2.3.2.4 Effect of different alcohols

In this study, transesterification was also carried out using different alcohols *viz*. methanol, ethanol and 1-propanol. The key objectives in varying alcohols in this study are to know the influences of different alcohols on the reaction and the efficacy of the catalyst in terms of reaction time and product yield. Individual reactions were carried out at the optimum reaction conditions (5 wt. % of trunk catalyst and 9:1 alcohol to oil ratio) at 65 °C. The results of the reaction are shown in **Fig. 2.14**. It has been found that with the increase in the number of

carbons in the alcohols used, the reaction time was found to be increased significantly from methanol to 1-propanol. Similarly, the biodiesel yields significantly decreased with increasing the number of carbons in the alcohols. The reaction with methanol in a short reaction time along with significantly good biodiesel yield is suggesting the suitability of methanol for biodiesel production. It has been reported that methanol is the most utilized alcohol for biodiesel production due to its low-cost and advantages of physical and chemical properties (Knothe, 2005; Takase et al., 2014). Ethanol is less toxic and easier for handling purposes than methanol, and it has some benefits for environmental and safety issues (Kanitkar et al., 2011; Yusoff et al., 2014). Methanolysis proceeds at a faster rate because of more nucleophilicity of methoxide ion in comparison to ethoxide ion in ethanolysis. There is a decrease in reactivity of nucleophiles as with the increase in the carbon chain length of the alkoxide ion. Butanolysis is a monophasic reaction and its initial rate of reaction is faster, but overall, it may result in a lower product yield of butyl esters compared to ethyl or methyl esters (Moser, 2009). Kanitkar et al. (2011) stated that methanol required lower alcohol to oil ratio compared to ethanol for biodiesel production, and mentioned that methanol performs better in terms of biodiesel conversion and yields. They also reported that the activation energy for methanol was found to be lower than that of ethanol that is indicating more energy efficiency for biodiesel production with methanol. A higher product of methyl biodiesel is obtained compared to ethyl biodiesel (Kanitkar et al., 2011). This may be due to the formation of the stable ethyl ester emulsions leading to difficulty in separation or extraction process and loss of the products in comparison to methyl biodiesel (Moser, 2009; Yusoff et al., 2014). It is evident that the physicochemical properties of biodiesel mainly depend on the type and composition of oils; the nature of the alcohol used does not have a significant effect on biodiesel properties (Bejan et al., 2014; Yusoff et al., 2014). Bejan et al. (2014) reported that transesterification reaction using benzyl alcohol yielded biodiesel with high density and kinematic viscosity values that do not meet the specifications of international biodiesel standards. In these contexts, methanol is still considered the leading alcohol for the production of biodiesel.

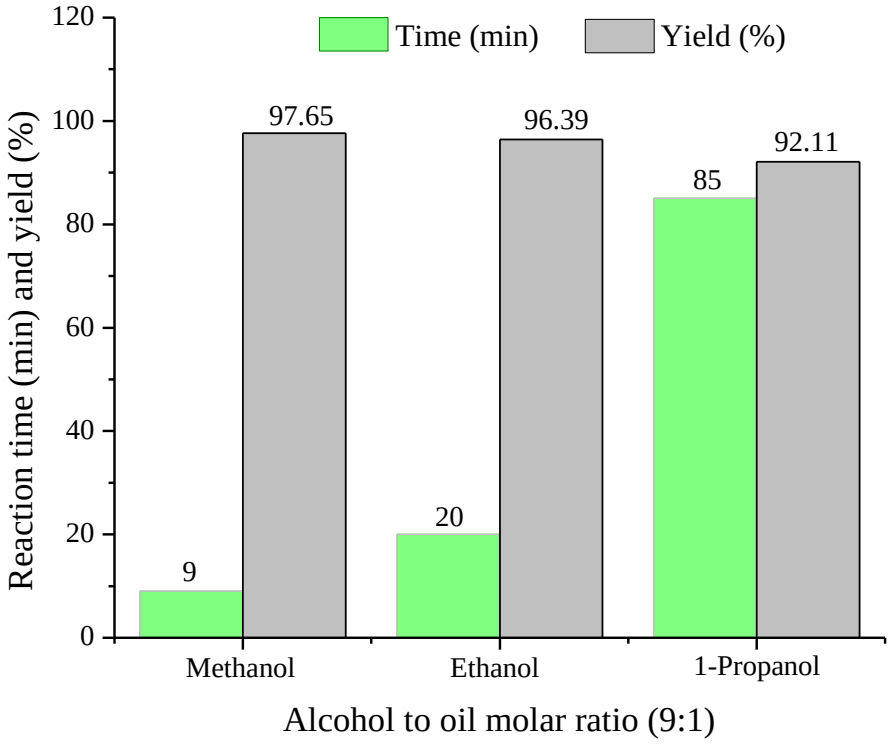

Fig. 2.14. Effect of different alcohols on biodiesel synthesis (Temperature = 65 ^{o}C, *M. paradisiaca* trunk catalyst loading = 5 wt.%).

2.3.2.5 Investigation of catalyst reusability

In this study, *M. paradisiaca* trunk catalyst considerably showed better activities and the reusability of this was investigated under the optimized conditions (5 wt. % catalyst, 9:1 MTOMR, and 65 ^{o}C). After completion of the reaction, the catalyst was filtered under the suction pump, and the recovered catalyst was washed four times with petroleum ether followed by acetone to remove the presence of any residual methyl ester products or glycerol. The recovered catalyst was dried for 4 h in the hot air oven at 110 ^{o}C, cooled in the desiccator, and the next reaction cycle was performed. A similar procedure was employed for every reaction cycle. The reusability data are depicted in **Fig. 2.15** and this revealed that the *M. paradisiaca* trunk catalyst could be successfully reused up to 3rd reaction cycle with a high biodiesel yield. In each reaction cycle, a gradual decrease in catalytic activity was noticed and this might be due to a slight loss of the catalyst or leaching of the active components during the process of catalyst recovery. These are in accordance with the reusability results reported in the works of Gohain et al. (2017) and Mendonça et al. (2019b). During the study, to observe morphological characters and leaching or loss of any active components, the 3rd recycled catalyst was analyzed using FESEM and EDX techniques. The FESEM images of the fresh catalyst (**Fig. 2.5** C) and

3rd recycled catalyst (**Fig. 2.6**, A–C) showed changes of morphological characters, and breakdown and formation of smaller agglomerated particles and sheet-like structures. The EDX results of fresh catalyst (**Fig. 2.5** D) and 3rd recycled catalyst (**Fig. 2.6**, D) are presented in **Table 2.2**. This indicated the leaching of potassium and is confirming the active role played by potassium in the reaction. To observe any changes of characters of the catalyst, the 3rd recycled catalyst was also analyzed using powder XRD and FT-IR techniques. XRD analyses of the fresh catalyst (**Fig. 2.2**, blue line) and 3rd recycled catalyst (**Fig. 2.2**, red line) displayed the decrease and disappearance of some of the intensities and peaks of K_2CO_3 in the XRD pattern of the 3rd recycled catalyst which is in agreement with the EDX report (**Fig. 2.6** D, **Table 2.2**). This is indicating the role of K_2CO_3 played in the transesterification. Some changes in the FT-IR spectrum (**Fig. 2.3**, red line) and decrease of FT-IR peak of carbonate (CO_3^{2-}) at 1491 and 1419 cm^{-1} that may be due to the K_2CO_3 was also observed in the 3rd recycled catalyst. The decrease in the catalytic activity of the trunk catalyst in the biodiesel synthesis is because of the reduction of active sites of the catalyst due to leaching or loss of potassium. Glycerol molecules may also do agglomeration on the catalyst surface (**Fig. 2.3**, weak IR peaks at 2925 and 2855 cm^{-1} due to C-H stretching vibration of glycerol molecule) which may block the active-sites and result in a reduced activity on the reuse of the catalyst.

Biodiesel contaminated with metals beyond the specified limit has some detrimental effects on its usage as a fuel for the diesel engine. Metals play the role of catalyst for oxidation of biodiesel (Jain et al., 2012; 2014), affect the storage stability of biodiesel (Jain et al., 2012), and can damage the devices of diesel engines used for controlling emissions (Schröder et al., 2017). To examine the contaminant elements, present in the biodiesel due to metal leaching from the catalyst, Na and K contents in biodiesel and *J. curcas* oil were tested using a Flame photometer (Systronics-128), and Ca and Mg contents were determined using AAS (Shimadzu-AA-6300). ASTM D6751 and EN 14214 biodiesel standards specified the maximum limit of 5 ppm for combined Na and K. It is very pleasant to report that 1.21 ppm of Na and 0.43 ppm of K could be detected in the biodiesel which is 1.64 ppm in total (Na + K), and well below the prescribed upper limit. *J. curcas* oil was also found to contain low levels of Na (0.42 ppm) and K (0.79 ppm). Negligible amounts of Ca (0.19 ppm) and Mg (0.08 ppm) were detected in *J. curcas* oil. No significant increase in the concentration of Ca (0.21 ppm) and Mg (0.09 ppm) was noticed in the produced biodiesel. It is notable to mention that the biodiesel produced in this study is not contaminated with alkali metals (Na + K) and alkaline earth metals (Ca + Mg).

Pathak et al. (2018) utilized a heterogeneous catalyst derived from *M. acuminata* peel in biodiesel synthesis. They investigated the reusability of catalyst and after the 4th run, significant

loss of K concentration from 70.06 % to 27.99 % and Ca from 9.54 % to 4.81 % was reported. Nath et al. (2019; 2020) studied the reusability of agro-wastes derived heterogeneous catalysts. In the 3rd recycled catalyst, they reported leaching of K from 15.13 % to 10.19 % in *Brassica nigra* catalyst and from 6.13 % to 1.14 % in *Sesamum indicum* catalyst. A substantial loss of K component from 19.05 wt. % to 6.00 wt. % in the 3rd recycled catalyst has been reported in the *Heteropanax fragrans* bio-waste derived heterogeneous base catalyst (Basumatary et al., 2021c). Sarma et al. (2014), Gohain et al. (2017), Aleman-Ramirez et al. (2021), and Arumugam and Sankaranarayanan (2020) have also reported significant leaching of active components during catalyst reusability of their biomass sources derived heterogeneous catalysts. Based on these reports, *M. paradisiaca* catalyst of the present study performed much better in terms of activity, reaction time and product yield.

The present banana catalyst is found to be highly efficient for biodiesel synthesis and superior compared to other reported biobased catalysts (**Table 2.7**). As the catalyst showed good stability and activity without any significant loss of yields in the reusability test, the catalytic system would be considered as a sustainable process for biodiesel synthesis. Banana is extensively produced worldwide. The banana gives fruits only once in its lifetime. Worldwide massive demand for banana fruits generates a huge amount of post-harvest banana residues. It has an extremely high potential to be developed as the catalyst for biodiesel synthesis at a large-scale. The present catalyst has the advantage of reducing the cost of produced biodiesel. As the solid catalyst is prepared from the renewable raw material, it is easy to handle, non-corrosive, and reusable, and is considered an environmentally friendly material.

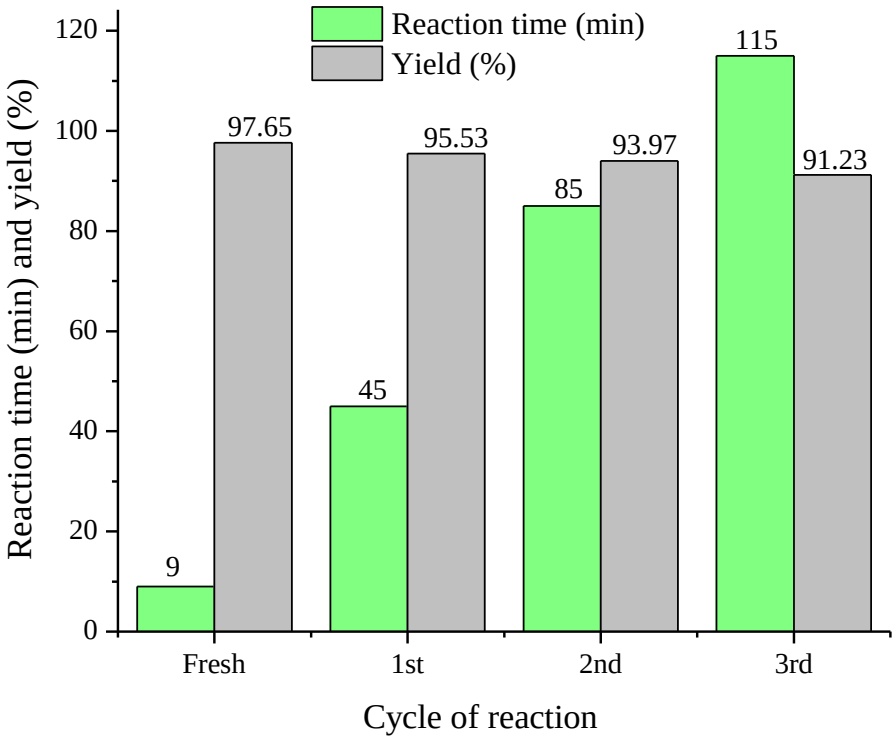

Fig. 2.15. Reusability of *M. paradisiaca* trunk catalyst calcined at 550 ^{o}C (Reaction temperature = 65 ^{o}C, MTOMR = 9:1, catalyst loading = 5 wt.%).

2.3.2.6 Activation energy of the reaction

Catalyst plays an active role in lowering the activation energy of a reaction, and accordingly, with low activation energy, the reaction occurs easily. In this study, the efficacies of *M. paradisiaca* peel, trunk and rhizome catalysts were investigated at different temperatures using optimized conditions. The rate constant (k) and activation energy (Ea) of all three catalysts were calculated following the reported equations (Nath et al., 2019). The Arrhenius plot of ln k versus 1/T (T–temperature in Kelvin) is depicted in **Fig. 2.16**, and Ea was determined from the slope of the straight line (Slope = - Ea/R; R–universal gas constant, 8.314 J K^{-1} mol^{-1}). The slopes of peel, trunk, and rhizome catalysts were found to be -5.8553, -5.7208 and -5.8848. Accordingly, the respective activation energy (Ea) was calculated as 48.68, 47.56, and 48.93 kJ mol^{-1}. Activation energies of the catalysts were found to be within the reported ranges of 21–84 kJ mol^{-1} for oil transesterification (Kumar and Ali, 2013; Kaur et al., 2018). Mendonça et al. (2019b) in the study of transesterification of soybean oil using *Astrocaryum aculeatum* catalyst reported the activation energy of 61.23 kJ mol^{-1} which is comparatively higher than the *M. paradisiaca* catalyst indicating more efficacy of this catalyst. It can be seen clearly from the Ea and slope values that the presented data are insignificant between the three different parts of the *M. paradisiaca* plant (peel, trunk and rhizome). The catalytic results

shown by these three catalysts (**Table 2.7**, 1st to 3rd row) are also matching with the basicity data. These data clearly show that the basicity and catalytic results among the three different catalysts are also non-significant. This study indicates that all the catalysts from the waste *M. paradisiaca* plant are contributing almost similar activities in the catalysis with remarkable efficacies. All the catalysts are showing almost equal importance in terms of their catalytic activities, activation energies, and potentialities. The reactions with activation energy in the range 10–15 kJ mol^{-1} are diffusion-controlled reactions and the reactions which have activation energies more than 25 kJ mol^{-1} are chemically controlled reactions (Kaur et al., 2018; Nath et al., 2019), and accordingly, the present biodiesel synthesis catalyzed by *M. paradisiaca* catalysts is chemically controlled reaction.

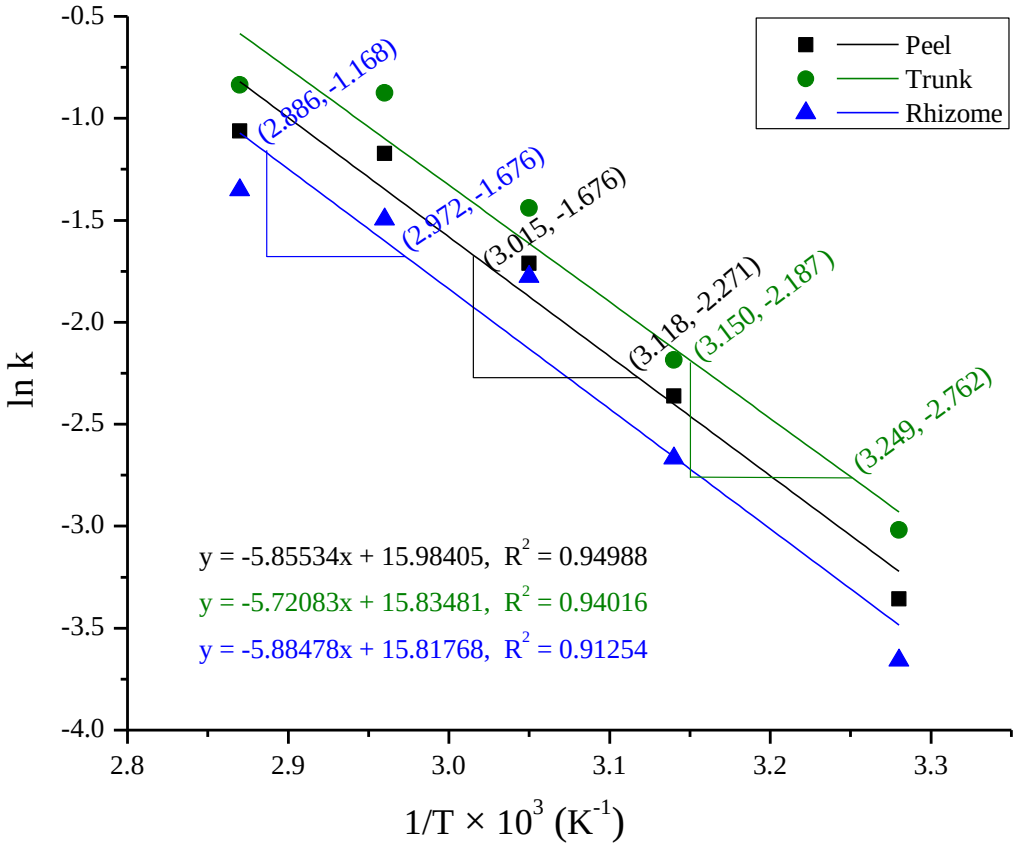

Fig. 2.16. Arrhenius plot of ln k versus 1/T (Reaction temperatures = 32, 45, 55, 65 and 75 ^{o}C).

2.3.3 Comparative catalytic activity with reported heterogeneous catalysts

In this work, the optimum conditions for biodiesel production using *M. paradisiaca* catalysts were studied and found to be 5 wt. % of catalyst amounts, 9:1 MTOMR, and reaction temperature of 65 ^{o}C. At these conditions, all the three calcined *M. paradisiaca* peel, trunk and rhizome catalysts exhibited nearly equal catalytic activities (**Fig. 2.13**). The burnt materials of peel, trunk and rhizome were also tested for their catalytic activities following similar reaction conditions and the results (**Fig. 2.17**) showed comparatively lower efficacies in catalysis than that of the calcined catalysts (**Fig. 2.13**). This may be due to the occurrence of lower K concentrations in the burnt materials (**Table 2.4**) in comparison to the calcined catalysts (**Table 2.2**). It is to be noted that the calcined trunk catalyst displayed slightly better catalytic activity for the reaction which yielded 97.65 % of biodiesel only in 9 min of reaction time (**Fig. 2.13**, **Table 2.7**). This result is due to its highest potassium content revealed from FESEM-EDX (**Fig. 2.5**, **Table 2.2**) and XPS (**Fig. 2.8**, **Table 2.5**) which is present in the form of K_2CO_3 and K_2O as the active components (**Fig. 2.2**, **Fig. 2.3**). A higher pH value in the trunk catalyst was also observed because of its higher K content compared to peel and rhizome catalysts (**Fig. 2.10**). The basicity of *M. paradisiaca* catalyst was found in the increasing order of 1.39 mmol g^{-1} (rhizome) < 1.43 mmol g^{-1} (peel) < 1.59 mmol g^{-1} (trunk). Accordingly, the catalysts exhibited catalytic efficiencies in a similar trend (**Table 2.7**) with TOF in the similar order of 46.16 min^{-1} (rhizome) < 56.85 min^{-1} (peel) < 68.24 min^{-1} (trunk). The heterogeneous catalyst from *M. paradisiaca* trunk is extremely basic and excellently contributing to the catalytic activity. It is seen from **Table 2.7** that heterogeneous base catalysts from various biomass sources were reported for biodiesel production by Deka and Basumatary (2011), Nath et al. (2020), Mendonça et al. (2019b), Odude et al. (2019), Betiku et al. (2016), Wang et al. (2017a), Pathak et al. (2018) and Kumar et al. (2016). In their works, lower catalytic activities were reported and this may be due to lower surface areas of these catalysts compared to the *M. paradisiaca* trunk catalyst whose surface area is comparatively higher. The better efficacy of *M. paradisiaca* trunk catalyst may also be due to its higher basic character. Nath et al. (2019) reported *B. nigra* catalyst for biodiesel synthesis with the comparable surface area. The present trunk catalyst is showing more efficiency than that of *B. nigra* catalyst which might be because of the higher K content and more basic character of the present catalyst. *M. paradisiaca* catalyst is found to be superior in the activity than the snail shell derived CaO catalyst with comparable surface area (Laskar et al., 2018) that might be due to its higher K content, and further, the oxide and carbonate of potassium are more basic than that of calcium. It is seen from **Table 2.7** that the catalysts from *M. balbisiana* rhizome (Sarma et al., 2014; Aslam et al., 2014), *L.*

perpusilla (Chouhan and Sarma, 2013), *A. nilotica* (Sharma et al., 2012), and *M. acuminata* peduncle (Balajii and Niju, 2019) showed lower catalytic activities. These are due to the presence of lower potassium concentrations in all these catalysts (**Table 2.3**). Relatively large surface areas (**Table 2.7**) and higher potassium concentrations (**Table 2.3**) were reported in the catalyst of *M. balbisiana* peel (Gohain et al., 2017), *C. papaya* stem (Gohain et al., 2020a), and *M. acuminata* peduncle (Balajii and Niju, 2019) without reporting the composition of C and/or O in some of these catalysts. As a result, the K concentrations in these catalysts might decrease and showed lower efficacies in comparison to *M. paradisiaca* catalysts where the percentage of C and O along with K and other elements were reported. Diverse types of biomass sources have been identified for the development of heterogeneous base catalysts. These are *Heteropanax fragrans* (Basumatary et al., 2021c), *Carica papaya* peel (Etim et al., 2021), *Citrus sinensis* peel ash@Fe_3O_4 (Changmai et al., 2021), sugarcane leaf residual ash (Arumugam and Sankaranarayanan, 2020), pineapple leaf (Barros et al., 2020), pawpaw peel (Oladipo et al., 2020) and *Moringa oleifera* leaf (Aleman-Ramirez et al., 2021). Longer reaction times have been reported to achieve high biodiesel yield with these heterogeneous catalysts compared to the catalysts reported in this study. Their catalytic activities are due to the existence of alkali metal components in the catalysts and mainly due to the concentration of K which is found to be lower in comparison to that of the present *M. paradisiaca* catalyst. Solid catalyst derived from a blend (equal proportions) of plantain peel and cocoa pod husk also displayed lower efficacy in biodiesel synthesis (Olatundun et al., 2020). In summary, it is noteworthy to mention that *M. paradisiaca* trunk catalyst performed very well and could produce 97.65 % yield of biodiesel under optimal conditions of 5 wt. % of catalyst and 9:1 MTOMR at 65 ^{o}C in only 9 min of reaction time. The catalyst due to its higher K content and more basic character exhibited superior and remarkable catalytic properties with a very fast rate of reaction amongst the other reported heterogeneous base catalysts (**Table 2.7**).

In this study to investigate the efficacy of the catalyst for biodiesel production, all the experiments were performed using 2 g of *J. curcas* oil. To study the fuel properties, several rounds of reactions were performed to prepare 1000 mL (1 L) biodiesel using 100 g of oil at a time under the optimized experimental conditions. It is interesting to mention that at the scale of 100 g oil, the biodiesel produced is high enough with a yield of 95 % and the reaction rate is found to be comparable to that of 2 g oil. This indicates that the catalyst has strong potential for the production of biodiesel on a large-scale for commercial purposes.

Table 2.7: Catalytic activity comparison of *M. paradisiaca* catalysts in biodiesel synthesis with reported agro-wastes derived ash-based catalysts.

Biodiesel feedstock	**Catalyst source (Ash)**	**Surface area ($m^2 g^{-1}$)**	**Parameters**				**Biodiesel, Y or C (%)**	**References**
			MTOMR	**Catalyst (wt. %)**	**Temp (ºC)**	**Time (min)**		
J. curcas oil	*M. paradisiaca* peel	4.1	9:1	5	65	12	97.56 (Y)	This work
J. curcas oil	*M. paradisiaca* trunk	6.4	9:1	5	65	9	97.65 (Y)	This work
J. curcas oil	*M. paradisiaca* rhizome	7.0	9:1	5	65	14	95.67 (Y)	This work
Thevetia peruviana oil	MB trunk	1.4	20:1	20	32	180	96 (Y)	Deka and Basumatary (2011)
Sunflower oil	*Sesamum indicum*	3.6	12:1	7	65	40	98.9 (Y)	Nath et al. (2020)
Soybean oil	Tucumã peels	1.0	15:1	1	80	240	97.3 (C)	Mendonça et al. (2019b)
Palm oil	Banana peel	4.4	3:2.4	4	65	65	99 (Y)	Odude et al. (2019)
Bauhinia monandra oil	Banana peel	4.4	7.6	2.75	65	69	98.5 (C)	Betiku et al. (2016)
Rapeseed oil	Gasified straw slag	1.2	12:1	20	200	480	95 (C)	Wang et al. (2017a)
Soybean oil	MA peel	1.4	6:1	0.7	32	240	98.95 (C)	Pathak et al. (2018)
J. curcas oil	SrO-MBUS	0.04	9:1	5	200	60	96 (Y)	Kumar et al. (2016)
Soybean oil	*Brassica nigra*	7.3	12:1	7	65	25	98.79 (Y)	Nath et al. (2019)
Thevetia peruviana oil	*Brassica nigra*	7.3	12:1	7	65	25	97.78 (Y)	Nath et al. (2019)

J. curcas oil	*Brassica nigra*	7.3	12:1	7	65	30	98.26 (Y)	Nath et al. (2019)
Soybean oil	Snail shell	7.0	6:1	3	28	420	98 (Y)	Laskar et al. (2018)
J. curcas oil	MBUS	38.7	9:1	5	275	60	98 (Y)	Sarma et al. (2014)
Mesua ferrea oil	MBUS	38.7	9:1	5	275	60	95 (C)	Aslam et al. (2014)
J. curcas oil	*Lemna perpusilla*	9.6	9:1	5	65	300	89.43 (Y)	Chouhan and Sarma (2013)
J. curcas oil	$CaCO_3$- *Acacia nilotica*	14.0	12:1	5	65	180	91.7 (C)	Sharma et al. (2012)
Waste cooking oil	MB peel	14.0	6:1	2	60	180	100 (C)	Gohain et al. (2017)
Waste cooking oil	*Carica papaya* stem	78.6	9:1	2	60	180	95.23 (C)	Gohain et al. (2020a)
Ceiba pentandra oil	MA peduncle	45.9	11.46:1	2.68	65	106	98.73 (C)	Balajii and Niju (2019)
J. curcas oil	*Heteropanax fragrans*	27.50	12:1	7	65	65	97.75 (Y)	Basumatary et al. (2021c)
Honne oil	Cocoa pod husk-plantain peel	18.86	15:1	4.5	65	150	98.98 (Y)	Olatundun et al. (2020)
WCO	*Carica papaya* peel	–	12:1	3.5	65	60	97.5 (Y)	Etim et al. (2021)
WCO	*Citrus sinensis* peel ash@Fe_3O_4	15.55	6:1	6	65	180	98 (Y)	Changmai et al. (2021)

Calophyllum inophyllum oil	Residual ash from sugarcane leaves	–	19:1	5	64	180	97 (Y)	Arumugam and Sankaranarayanan (2020)
Soybean oil	Pineapple leaves	–	40:1	4	60	30	98 (Y)	Barros et al. (2020)
Moringa oleifera oil	Pawpaw peel	3.6	9:1	3.5	35	40	96.43 (Y)	Oladipo et al. (2020)
Soybean oil	*Moringa oleifera* leaves	–	6:1	6	65	120	86.7 (Y)	Aleman-Ramirez et al. (2021)

MTOMR–methanol to oil ratio; wt–weight; min–minute; Temp–temperature; C–conversion; Y–yield; WCO–Waste cooking oil; MBUS–*Musa balbisiana* underground stem; MB–*Musa balbisiana*; MA–*Musa acuminata.*

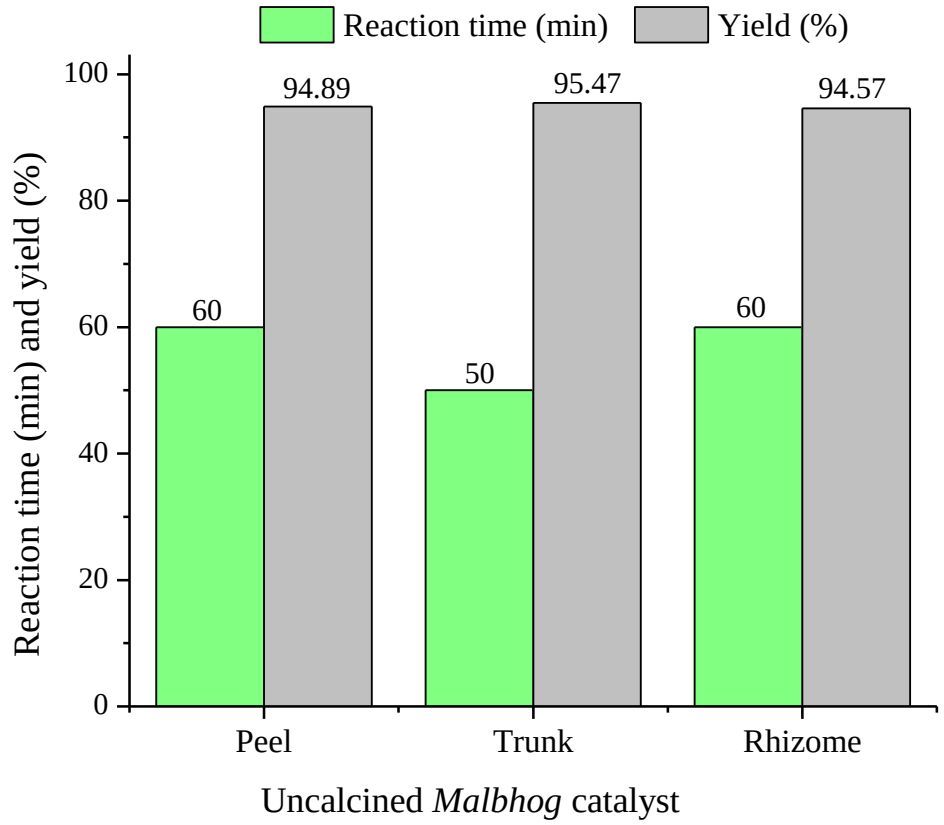

Fig. 2.17. Catalytic activities of the *M. paradisiaca* burnt materials in biodiesel production. Reaction conditions: Temperature = 65 ^{o}C, MTOMR = 9:1, catalyst loading (*M. paradisiaca* peel, trunk and rhizome) = 5 wt. %.

2.3.4 Characterization of jatropha biodiesel

2.3.4.1 FT-IR and NMR analyses

The strong peak at 1746 cm^{-1} is due to stretching vibration of the carbonyl (C=O) group of J. *curcas* oil which changes to 1743 cm^{-1} due to the C=O group of methyl esters indicating the transformation of *J. curcas* oil to biodiesel (**Fig. 2.18**). The absorption peak at 3009 cm^{-1} in oil and 3008 cm^{-1} in biodiesel represents =C–H stretching frequencies of the fatty acid chains of triglyceride and biodiesel. The signals due to C–H stretching vibrations are observed at 2928 and 2853 cm^{-1} in the *J. curcas* oil, and 2926 and 2855 cm^{-1} in the product. The terminal CH_3 bending vibrations are represented by the peaks at 1461 and 1381 cm^{-1} in the *J. curcas* oil, and at 1461, 1437 and 1363 cm^{-1} in the biodiesel. The C–O stretching bands of triglyceride and methyl ester molecules appeared at 1236, 1157 and 1098 cm^{-1} in the *J. curcas* oil, and at 1245, 1196, 1176 and 1018 cm^{-1} in the product. The IR signal at 724 cm^{-1} both in the oil and biodiesel indicated the $–CH_2–$ rocking of the long chains (fatty acid moiety).

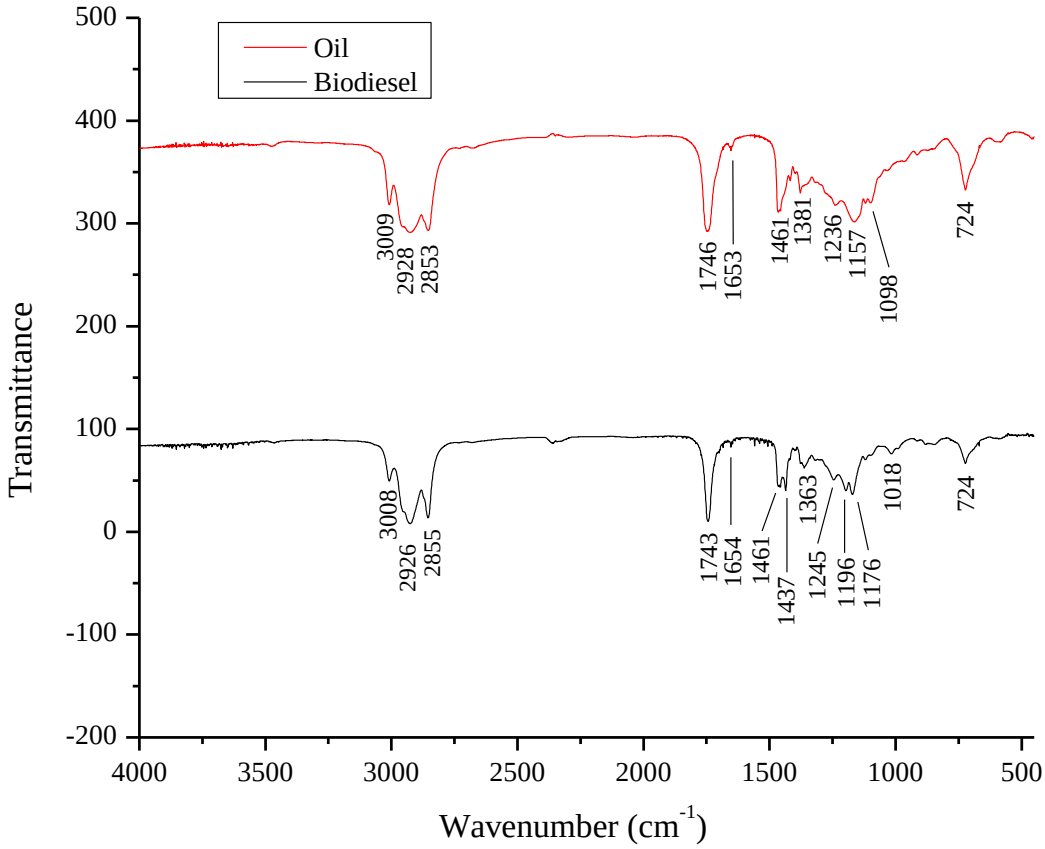

Fig. 2.18. FT-IR spectra of *J. curcas* oil and biodiesel.

The *J. curcas* oil and biodiesel were characterized from ^{1}H NMR (**Fig. 2.19**, **Fig. 2.20**) and ^{13}C NMR spectra (**Fig. 2.21**, **Fig. 2.22**) to confirm the transformation of *J. curcas* oil to biodiesel. Various types of protons and carbons are interpreted from the NMR spectra and signified in **Table 2.8**. The ^{1}H NMR signals due to methine proton at C2 of triglycerides (-C***H***-CO_2R) at δ 5.254–5.293 ppm, and methylene protons at C1 and C3 of triglycerides (-C***H***$_2$-CO_2R) at δ 4.122–4.166 ppm (dd, ^{3}J = 5.8, 11.8 Hz) and δ 4.278–4.318 ppm (dd, ^{3}J = 4.2, 11.8 Hz) in the *J. curcas* oil (**Fig. 2.19**) is completely disappearing in the ^{1}H NMR spectrum of jatropha biodiesel (**Fig. 2.20**). A new singlet signal at δ 3.66 ppm due to the methoxy protons (-CO-OC***H***$_3$) is observed in the ^{1}H NMR spectrum (**Fig. 2.20**) indicating the complete conversion of oil to biodiesel. The disappearance of the signal at δ 68.897 ppm due to methine carbon at C2 of triglyceride (-***C***H-CO_2R) and δ 62.105 ppm due to methylene carbons at C1 and C3 of triglyceride (-***C***H$_2$-CO_2R) from the ^{13}C NMR spectrum of oil (**Fig. 2.21**), and appearance of a new signal at δ 51.416 ppm due to methoxy carbon (-CO-O***C***H$_3$) of methyl esters in the ^{13}C NMR spectrum of biodiesel (**Fig. 2.22**) also established the complete

transformation of oil to biodiesel. In this study, *J. curcas* oil was transesterified using ethanol also, and the produced biodiesel product i.e. FAEE (fatty acid ethyl esters) was recorded for ^{1}H NMR spectrum (**Fig. 2.23**, **Table 2.8**). The appearance of signals in the ^{1}H NMR spectrum (**Fig. 2.23**) at δ 4.096–4.149 ppm due to –OC***H***$_2$CH$_3$ (Quartet, 2H, –OC***H***$_2$–) indicated the complete formation of FAEE.

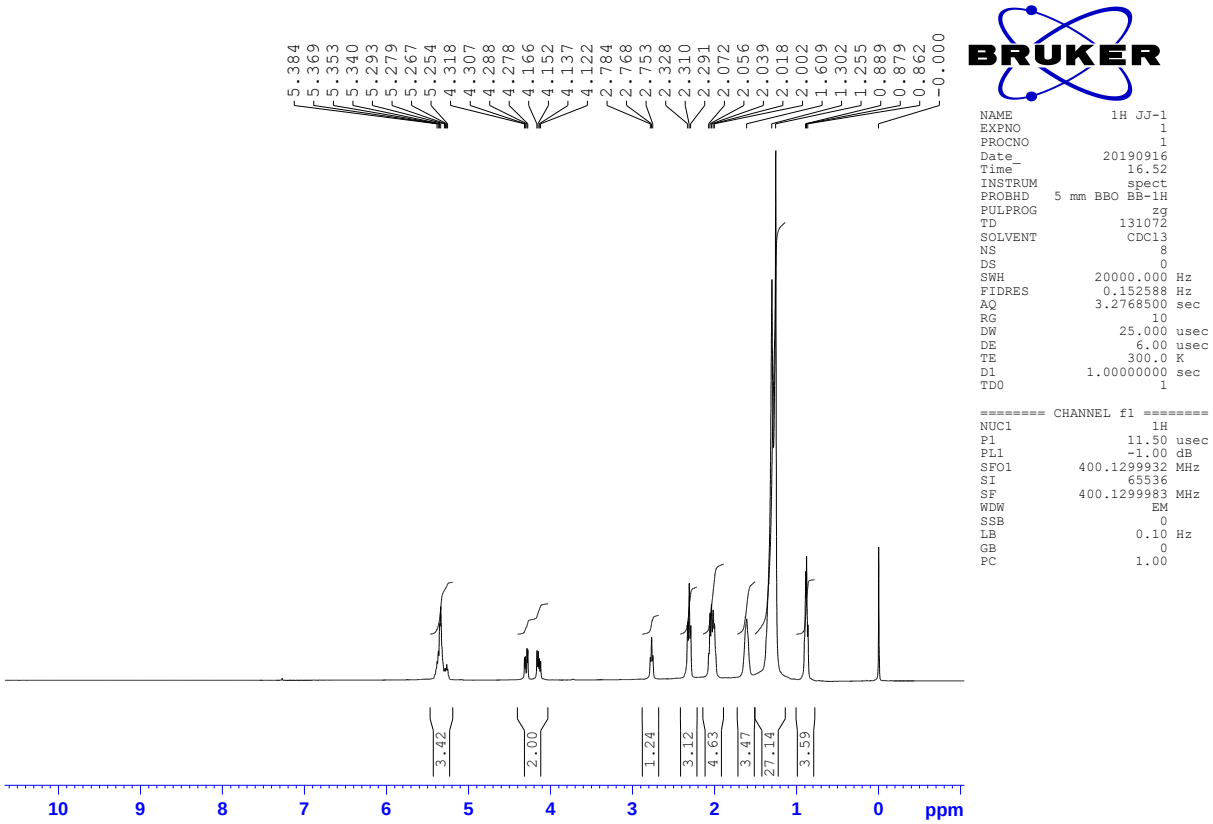

Fig. 2.19. ^{1}H NMR spectrum of *J. curcas* oil.

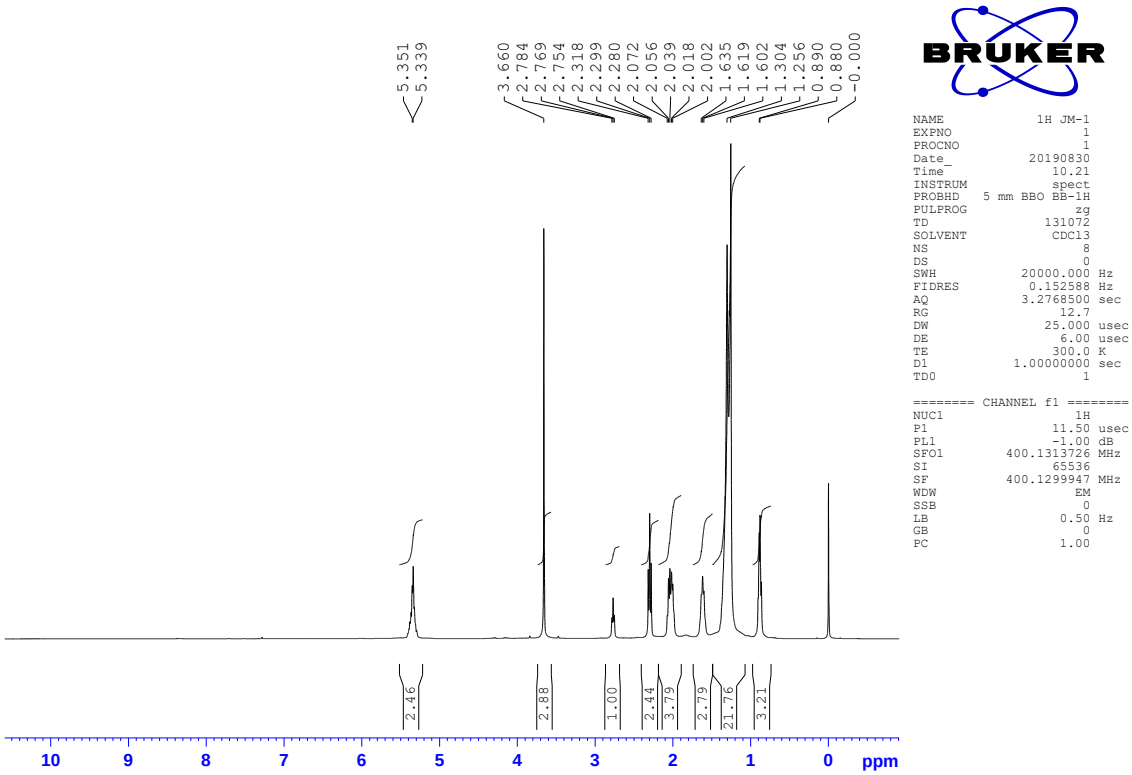

Fig. 2.20. ^{1}H NMR spectrum of jatropha biodiesel.

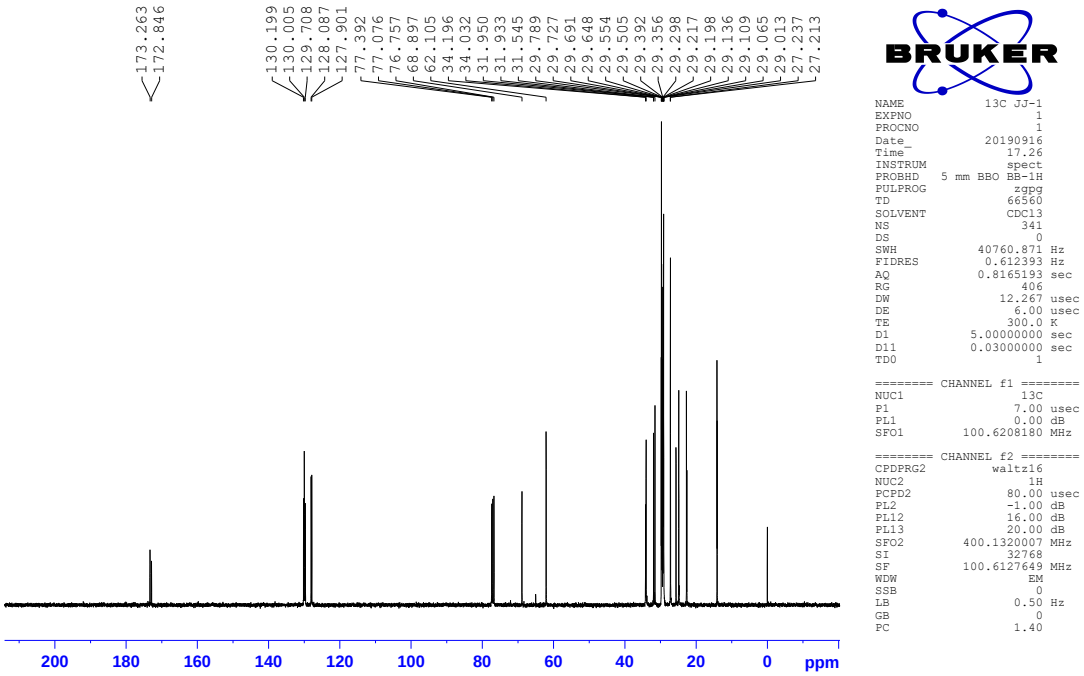

Fig. 2.21. ^{13}C NMR spectrum of *J. curcas* oil.

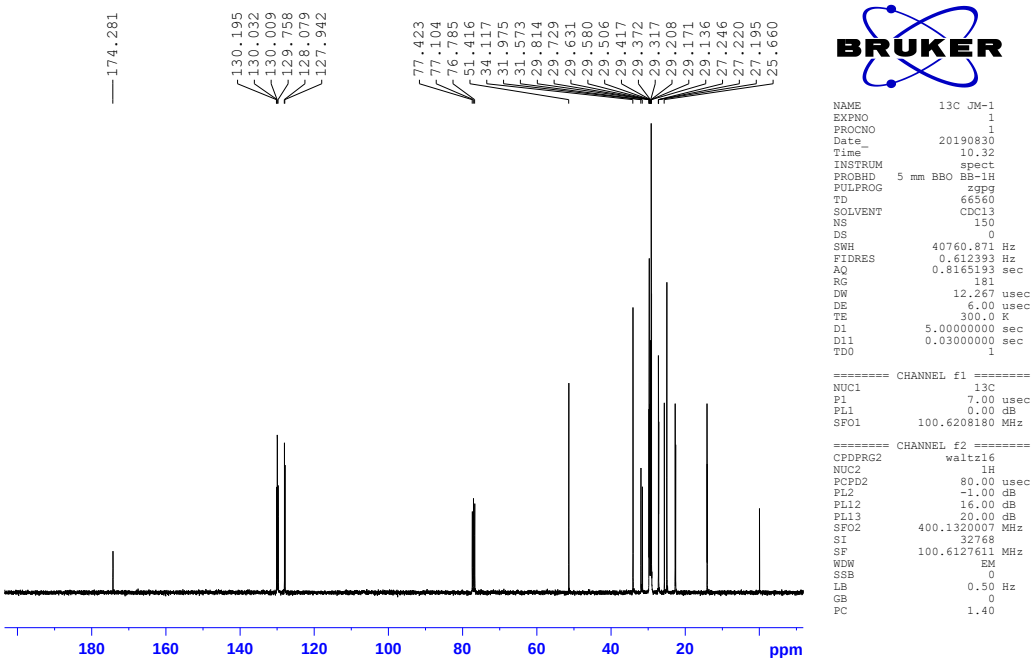

Fig. 2.22. ^{13}C NMR spectrum of jatropha biodiesel.

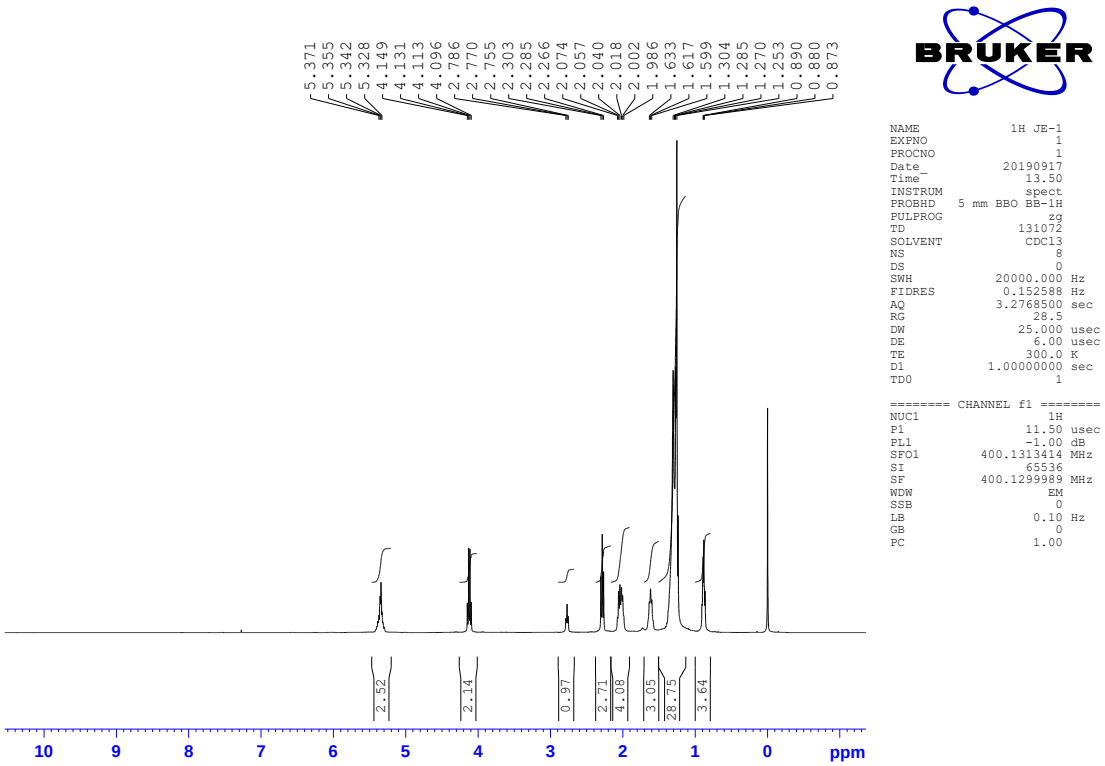

Fig. 2.23. ^{1}H NMR spectrum of jatropha biodiesel synthesized using ethanol (FAEE, fatty acid ethyl esters).

Table 2.8: NMR spectra analyses of *J. curcas* oil and biodiesel.

Types of protons/carbons	**Triglyceride (*J. curcas* oil)**		**Biodiesel (FAME)**		**Biodiesel (FAEE)**
	^{1}H (δ, ppm)	**^{13}C (δ, ppm)**	**^{1}H (δ, ppm)**	**^{13}C (δ, ppm)**	**^{1}H (δ, ppm)**
Carbonyl (C=O)	–	172.846–173.263	–	174.281	–
Olefinic protons/carbons (-CH=CH-)	5.340–5.384	127.901–130.199	5.339–5.351	127.942–130.195	5.328–5.371
Methine proton/carbon at C2 of glycerides (-CH-CO_2R)	5.254–5.293	68.897	–	–	–
Methylene protons/carbon at C1 and C3 of glycerides (-CH_2-CO_2R)	4.122–4.318	62.105	–	–	–
Methoxy protons/carbon (-$COOCH_3$) of esters	–	–	3.660	51.416	(4.096, 4.113, 4.131, 4.149)[a*]
Bis-allylic protons/carbon (-C=C-CH_2-C=C-)	2.753–2.782	–	2.754–2.784	–	2.755–2.786
α-methylene to ester (-CH_2-CO_2R)	2.291–2.328	–	2.280–2.318	–	2.266–2.303
α-methylene to double bond (-CH_2-C=C-)	2.002–2.072	–	2.002–2.072	–	1.986–2.074
β-methylene to ester (CH_2-C-CO_2R)	1.609	–	1.602–1.635	–	1.599–1.633
Backbone methylenes -$(CH_2)_n$-	1.255–1.302	22.602–34.196	1.256–1.304	22.604–34.117	1.253–1.304
Terminal methyl protons/carbon (C-CH_3)	0.862–0.889	14.108, 14.154	0.880–0.890	14.156	0.863–0.890

FAME–Fatty acid methyl esters; FAEE–Fatty acid ethyl esters; [a*]–OC***H***$_2$$CH_3$ (Quartet, 2H, –OC***H***$_2$–).

2.3.4.2 GC-MS analysis

A total of six different fatty acid methyl esters (FAME) present in the produced jatropha biodiesel identified from GC chromatogram (**Fig. 2.24**) following the library search with TurboMass software are displayed in **Table 2.9**. Methyl esters of the three unsaturated fatty acids such as methyl palmitoleate, methyl oleate, and methyl gondoate were found to be present in the biodiesel. Three methyl esters of saturated fatty acids *viz.* methyl palmitate, methyl stearate and methyl arachidate were also detected. Methyl oleate with the highest percentage was found to be the dominant FAME followed by methyl palmitate and methyl stearate.

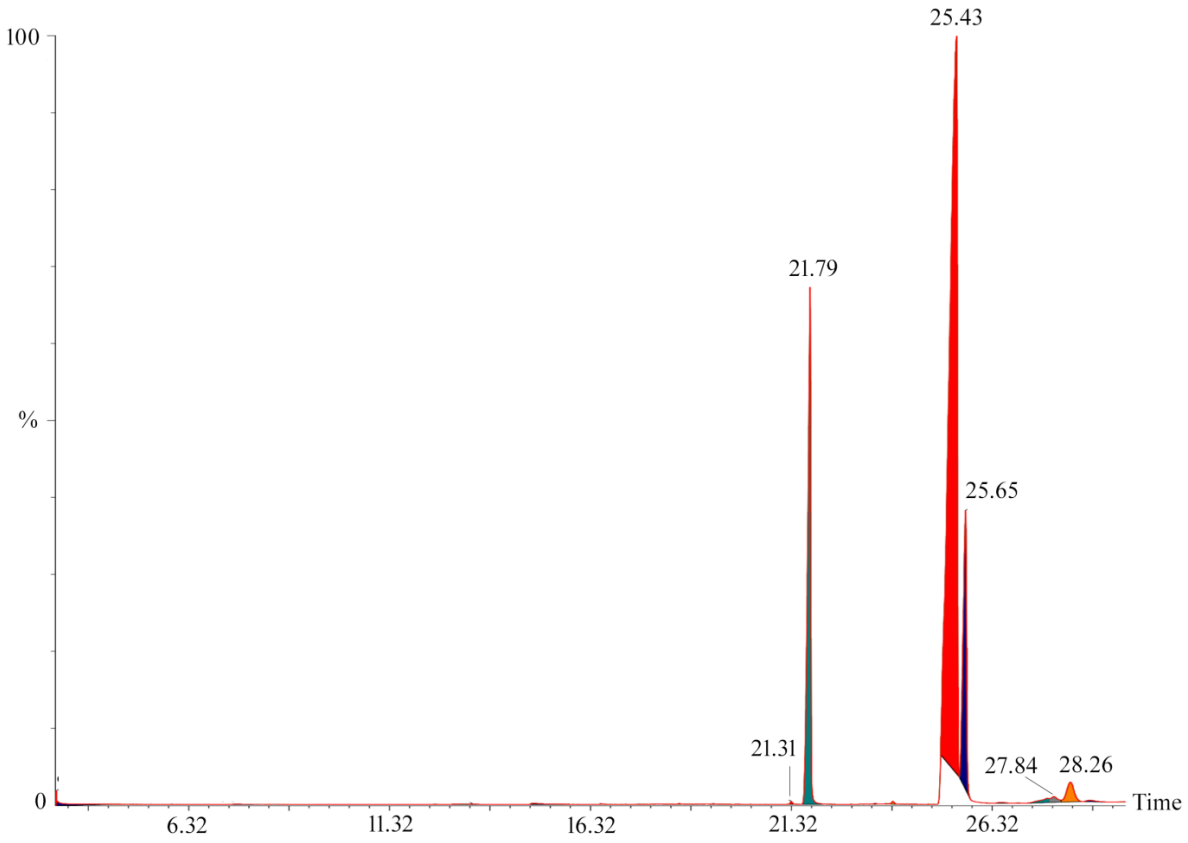

Fig. 2.24. GC chromatogram of jatropha biodiesel.

Table 2.9: Composition of jatropha biodiesel.

RT	FAME (Fatty acid methyl esters)	Composition (%)
21.31	Methyl palmitoleate (C16:1)	0.101
21.79	Methyl palmitate (C16:0)	17.90
25.43	Methyl oleate (C18:1)	66.429
25.65	Methyl stearate (C18:0)	10.995
27.84	Methyl gondoate (C20:1)	0.441
28.26	Methyl arachidate (C20:0)	1.713

2.3.5 Jatropha biodiesel properties

The different fuel properties of the produced jatropha biodiesel and comparison with international standards and reported biodiesels are summarized in **Table 2.10**. The density of the jatropha biodiesel was found within the prescribed limit of EN 14214, and comparable with the values of other reported biodiesels. The kinematic viscosity of the jatropha biodiesel at 40 ^{o}C was determined to be 3.799 $mm^2 s^{-1}$ which is within the range of ASTM D6751 and EN 14214, and far better than the values reported by Betiku and Ajala (2014), and Chouhan and Sarma (2013). It has been reported that low kinematic viscosity is preferable for good combustibility and non-deposition in the engine (Deka and Basumatary, 2011; Nath et al., 2019). The cetane index of jatropha biodiesel was calculated as 61.48 which is higher compared to the cetane index of soybean biodiesel reported by Nath et al. (2019). The cetane number obtained was 55.2 for jatropha biodiesel which is higher than the prescribed limit of the international standards (ASTM D6751 and EN 14214), and comparatively better than the value of 48.6 for the jatropha biodiesel reported by Sarma et al. (2014). The saponification number (SN) of the biodiesel was found to be 192.03 mg KOH/g, which is close to the value of sunflower biodiesel reported by Nath et al. (2020). The unsaturation present in the jatropha biodiesel represented by the iodine value was calculated as 58.87 g I_2/100 g which is favorable and far below the maximum value prescribed by EN 14214 standard. High iodine values were reported in the works of Nath et al. (2019), Aslam et al. (2014), Betiku and Ajala (2014), and Sarma et al. (2014). Other biodiesel properties like diesel index, aniline point, and American petroleum index were found to be 71.50, 208.58, and 34.25. The higher heating value (HHV) of 40.67 MJ/kg was obtained for the present biodiesel. The pour point and CFPP (cold filter plugging point) of the biodiesel were determined as -6 and -3. The comparative study of

properties (**Table 2.10**) reveals that the produced biodiesel fulfills the fuel properties of international standards and is found to be comparable to that of the reported biodiesels. The metals like Na, K, Ca and Mg were tested to examine the contaminant levels in the biodiesel due to metal leaching from the catalyst. It is very pleasant to mention that 1.21 ppm of Na and 0.43 ppm of K could be detected in the biodiesel which is 1.64 ppm in total (Na + K), and well below the prescribed upper limit (**Table 2.10**). Negligible amounts of Ca (0.21 ppm) and Mg (0.09 ppm) were detected in the produced biodiesel and these are within the specified limit. These results demonstrate that the biodiesel produced in this study is not contaminated with alkali metals (Na + K) and alkaline earth metals (Ca + Mg). Chouhan and Sarma (2013), Sarma et al. (2014), and Betiku et al. (2019) utilized biowastes derived heterogeneous catalysts in biodiesel synthesis. Though leaching of some metals from the catalysts was reported, concentrations of metals in their biodiesel were also found within the specified range.

Table 2.10: Properties of jatropha biodiesel and comparison with standards and reported biodiesels.

Properties	**Jatropha biodiesel** (This work)	**ASTM D6751**	**EN 14214**	**Reported biodiesels**								
				Soybean oil (Nath et al., 2019)	***Kariya* oil** (Betiku et al., 2019)	**WCO** (Gohain et al., 2020b)	***Thevetia peruviana* oil** (Betiku and Ajala, 2014)	**WCO** (Gohain et al., 2017)	***Mesua ferrea* oil** (Aslam et al., 2014)	**Sunflower oil** (Nath et al., 2020)	***J. curcas* oil** (Sarma et al., 2014)	***J. curcas* oil** (Chouhan and Sarma, 2013)
Density at 15 ^{o}C (g/cm^3)	0.866	NS	0.86–0.90	0.861	0.896	0.85	0.887	0.89	0.873	0.859	0.875	0.891
Kinematic viscosity at 40 ^{o}C (mm^2/s)	3.799	1.9–6.0	3.5–5.0	3.76	5.6113	4.15	6.0	3.12	5.525	3.11	5.7	6.8
Cetane number	55.2	47 (min)	51 (min)	56.67	54.94	58	123.25	55	-	53.95	48.6	-
Cetane index	61.48	NS	NS	56.13	-	-	-	-	-	-	-	-
Pour point (^{o}C)	-6	NS	NS	-3	-	-9	+1	-9	-	-6	3	-
CFPP (^{o}C)	-3	NS	NS	0	-	-	-	-	-	-3	-	-

SN (mg KOH/g)	192.03	NS	NS	176.33	-	-	-	-	-	188.57	-	-
Iodine value (g I_2/100 g)	58.87	NS	120 (max)	121.91	-	-	90.23	-	113.24	-	119	-
API	34.28	36.95	NS	32.756	-	-	28.03	-	-	34.277	0.875	0.892
Diesel index	71.50	50.4	NS	55.309	-	-	157.29	-	-	50.82	-	-
Aniline point (^{o}F)	208.58	331	-	168.85	-	-	-	-	-	148.27	-	-
HHV (MJ/kg)	40.67	NS	NS	40.37	39.05	39.32	-	40.20	35	39.79	39.25	37.100
Na (ppm)	1.21	(Na +	(Na +	-	1.8	-	-	-	-	-	5.0	4.0
K (ppm)	(0.42)[a]	K)	K)									
	0.43	5 (max)	5									
	(0.79)[a]		(max)									
Ca (ppm)	0.21	(Ca +	(Ca +	-	0.42	-	-	-	-	-	-	-
Mg (ppm)	(0.19)[a]	Mg)	Mg)									
	0.09	5 (max)	5									
	(0.08)[a]		(max)									

WCO–Waste cooking oil; NS–Not specified; max– maximum; min– minimum; CFPP–Cold filter plugging point; SN–Saponification number; API–American petroleum index; HHV–Higher heating value; [a], metal content in *J. curcas* oil.

2.4 Conclusions

In this work, highly efficient, recyclable, and renewable heterogeneous base catalysts derived from *M. paradisiaca* peel, trunk, and rhizome for biodiesel production from *J. curcas* oil have been reported. The characterization of XRD and FESEM-EDX indicated the existence of potassium as K_2CO_3, KCl and K_2O, and high K concentrations in all three catalysts. The analyses of BET, FESEM, and HRTEM revealed that the *M. paradisiaca* catalysts consisted of characters of porous materials of micro-mesoporosity nature. The Hammett method confirmed the basicity in the order of 1.39 mmol g^{-1} (rhizome) < 1.43 mmol g^{-1} (peel) < 1.59 mmol g^{-1} (trunk). The high biodiesel yield of 97.65 % could be explained based on the high basicity of *M. paradisiaca* trunk catalyst under the reaction conditions of 9:1 MTOMR and 5 wt. % of catalyst loads at 65 ^{o}C, and trust that this would be the first report in the shortest reaction time of 9 min. The catalyst was reused successfully up to the 3rd reaction cycle exhibiting a good biodiesel yield (91.23 %) with little loss of catalytic activity due to leaching of potassium during the recycling process. The trend of catalytic efficiencies of all the catalysts is matching with the basicity and TOF that was also found in the order of 46.16 min^{-1} (rhizome) < 56.85 min^{-1} (peel) < 68.24 min^{-1} (trunk). The metals like Na, K, Ca and Mg in ppm levels were detected in the biodiesel and well below the upper limit prescribed in the biodiesel standards. The raw materials being easily available can be obtained free of cost from the post-harvest *M. paradisiaca* wastes for the catalyst preparation. *M. paradisiaca* wastes will provide a low-cost heterogeneous base catalyst with ease of handling, non-toxicity, biodegradability and reusability for efficient biodiesel production at a large-scale."